Open access • Posted Content • DOI:10.1101/2020.09.02.279406

Defining human mesenchymal and epithelial heterogeneity in response to oral inflammatory disease — Source link

Ana J Caetano, Val Yianni, Ana Angelova Volponi, Veronica Booth ...+2 more authors

Institutions: King's College London, University of Bedfordshire

Published on: 02 Sep 2020 - bioRxiv (Cold Spring Harbor Laboratory)

Topics: Tissue homeostasis and Mesenchymal stem cell

Defining human mesenchymal and epithelial heterogeneity in response to oral inflammatory disease

Ana J. Caetano [1*], Val Yianni [1*], Ana A. Volponi[1], Veronica Booth[2], Eleanor M. D'Agostino [3], Paul T. Sharpe[1]

1. Centre for Craniofacial and Regenerative Biology, Faculty of Dentistry, Oral & Craniofacial Sciences, King's College London, London, SE1 9RT

2. Department of Periodontology, Faculty of Dentistry, Oral & Craniofacial Sciences, King's College London, London, SE1 9RT

3. Unilever R&D, Colworth Science Park, Sharnbrook, Bedfordshire, MK44 1LQ

* Equal contributions

Correspondence to Paul T. Sharpe:

Centre for Craniofacial and Regenerative Biology
Faculty of Dentistry, Oral & Craniofacial Sciences
Floor 27, Tower Wing
Guy's Hospital
London SE1 9RT
(+44) 0207 188 8308
paul.sharpe@kcl.ac.uk

Conflict of interest: The authors have declared that no conflict of interest exists. However, E. D'A is an employee of Unilever Plc. This work was funded by Unilever in the form of a research grant awarded to P.T.S

Abstract

Human oral soft tissues provide the first barrier of defence against chronic inflammatory disease and hold a remarkable scarless wounding phenotype. Tissue homeostasis requires coordinated actions of epithelial, mesenchymal and immune cells. However, the extent of heterogeneity within the human oral mucosa and how tissue cell types are affected during the course of disease progression is unknown. Using single cell transcriptome profiling we reveal a striking remodelling of the epithelial and mesenchymal niches with a decrease in functional populations that are linked to the aetiology of the disease. Analysis of ligand-receptor interaction pairs identify potential intercellular hubs driving the inflammatory component of the disease. Our work establishes a reference map of the human oral mucosa in health and disease, and a framework for the development of new therapeutic strategies.

Key words:

human oral mucosa, periodontitis, oral mesenchymal cells, oral epithelial cells

Introduction

The oral mucosa is one of the most rapidly dividing tissues in the body and provides the first line of defence against the development of oral disease. Gingiva is the oral mucosa that surrounds the cervical portion of the teeth, and consists of a keratinised stratified squamous epithelium and an underlying connective tissue containing multiple cell types that collectively orchestrate tissue homeostasis during health and in response to mechanical and microbial challenges (Lindhe et al., 2008, Cekici et al., 2014). Periodontal disease is a chronic inflammatory condition associated with a dysbiosis of the commensal oral microbiota and host immune defences causing irreversible destruction of the soft and hard supporting tissues of the teeth (Pihlstrom et al., 2005, Lindhe et al., 2008). Gingivitis is a mild and reversible inflammation of the gingiva that does not permanently compromise the integrity of the tissues supporting the teeth. Chronic periodontitis occurs when untreated gingivitis progresses to the loss of the gingiva, bone and ligament (Lamont and Hajishengallis, 2015, Pihlstrom et al., 2005, Lindhe et al., 2008). Regenerating lost tissues remains the fundamental therapeutic goal and to achieve this it is necessary to understand the mechanisms and pathways controlling disease progression while identifying novel candidates for intervention.

Most studies on the pathogenesis of periodontal disease have largely focused on characterising the microbial biofilm and host immune response (Hajishengallis, 2014, Yucel-Lindberg and Bage, 2013). However, it is recognised that tissue resident cells play an instrumental role in innate immunity, immune regulation, and epithelial barrier maintenance (Krausgruber et al., 2020). Additionally, individual molecules known to play important roles in disease pathogenesis and the cell types they originate from remain ill-defined (Yucel-Lindberg and Bage, 2013).

Here we set out to unbiasedly profile human gingiva, including epithelial, mesenchymal and immune compartments using single cell RNA sequencing. To better characterise the dynamics of disease progression we used samples isolated from healthy and diseased patients. Our single-cell analysis identified differences in the composition of cellular sub populations residing within the gingival tissues and changes in the transcriptional fingerprint between healthy and diseased patient samples. We showed that these changes correlate with progressive diseased states. Despite the growing recognition that mesenchymal (stromal) cells maintain epithelial barrier integrity and immune homeostasis in several organs (Kabiri et al., 2014, Nowarski et al., 2017, Bernardo and Fibbe, 2013), the identity of gingiva-specific mesenchymal subtypes and the molecular attributes that regulate niche maintenance or disease remodelling have not been described. Significantly, we identified specific changes in mesenchymal cell populations indicative of playing a role in disease progression.

Intercellular network reconstruction in healthy and diseased states revealed loss of cell communication and increased immune interactions between the identified cell types. We provide novel insights into altered communication patterns between epithelial and mesenchymal cells caused by the inflammatory response.

Taken together, our data characterise the cellular landscape and intercellular interactions of the human gingiva, which enables the discovery of previously unreported cell populations contributing to oral chronic disease. Understanding the crucial roles of individual cell states during disease progression will contribute to the development of targeted cell-based approaches to promote regeneration or reduce inflammation-associated tissue dysfunction.

Results

Generation of the gingival transcriptional landscape in health and periodontitis.

Similar to other tissues in the gastrointestinal tract, the oral mucosa is a good model for studying a rapidly renewing tissue. To provide an in-depth analysis of cellular architecture, cell heterogeneity and understand gingival cell dynamics when transitioning from health to disease, we transcriptionally profiled single cells derived from patients. We obtained freshly resected human gingival tissue and isolated live cells (Figure S5) to be sequenced on the 10x Genomics Chromium platform for single cell RNA-seq (scRNA-seq) (Figure 1A). A total of 12,411cells were captured across four patient biopsies, allowing us to perform an in-depth analysis of single-cell transcriptomics. In order to ascertain the extent of likely human variation between datasets we first compared data from two healthy patients. Cells from these healthy patients were remarkably similar (Figure S1) and we observed a strong linear relationship in gene signatures between the two patient samples (Figure S1). Having established a high concordance of datasets obtained from two biopsies of healthy gingiva and to amplify the power of the study, these were merged and handled together for the subsequent analysis.

Carrying out a comparative bioinformatic analysis of samples obtained from healthy and periodontitis patients revealed a diversity in epithelial, stromal, endothelial and immune cells. A total of 16 distinct transcriptomic signatures were detected that corresponded to cell types or sub-populations of identifiable cell states. These were visualised using UMAP (Figure 1B).

In the epithelial compartment, we identified 3 subsets (clusters 1, 8 and 12), potentially corresponding to distinct differentiation stages. Cluster 1 shows a basal cell state with expression of *HOPX*, *IGBP5* and *LAMB3*; and cluster 8 a more mature cell state with

123 expression of *KRT1*, *KRT8*, *LAT* (Linker for Activation of T cells) and *PTGER* both
124 required for TCR (T-cell antigen receptor) signalling (Figure 1B, C; Figure S2).
125 Proliferating basal cells were identified in cluster 12 by expression of canonical marker
126 genes of proliferating cells such as *MKI67* and *TOP2A* (Whitfield et al., 2006) (Figure
127 1B, C; Figure S2). We also identify a mesenchymal (stromal-fibroblast) (cluster 6)
128 based on collagen expression; 1 perivascular (cluster 10) by high expression of
129 *PDGFRB* and *RGS5* (Figure 1B, C; Figure S2); 2 endothelial (clusters 9 and 15) in
130 which cluster 9 specifically expresses *CLDN5* and *EMCN* and cluster 15 shows high
131 expression of genes involved in the regulation of angiogenesis such as *KDR*, *TIE1*
132 and *SOX18* (Jones et al., 2001, Francois et al., 2008) (Figure 1B, C; Figure S2).
133 We identified immune clusters of the myeloid (macrophages and dendritic cells) and
134 lymphoid (T and B cells) lineages. B cells are shown in 3 distinct populations (clusters
135 0, 5 and 7) with clusters 0 and 5 expressing *MZB1*, *DERL3* and *IGHG4* characteristic
136 of follicular and IgG plasma B cells respectively, and cluster 7 expressing *MS4A1* and
137 *CD37* corresponding to memory B cells (Akkaya et al., 2020, James et al., 2020)
138 (Figure 1B, C; Figure S2). T cells are shown in cluster 3 identified by expression of
139 canonical TRM marker *CXCR6*. Dendritic cells of myeloid origin with high expression
140 of *CLEC9A* and *IRF8* are found in clusters 13 and 14 (Eisenbarth, 2019, James et al.,
141 2020), and mast cells are indicated in cluster 2 expressing *TPSB2* and *TPSB1*
142 (Abraham and St John, 2010) (Figure 1B, C; Figure S2). Macrophages are found in
143 two populations (clusters 4 and 11) sharing high expression of *LYZ* and *AIF1*
144 (Chakarov et al., 2019) (Figure 1B, C; Figure S2).
145 Together, these data provide the first detailed molecular insight into gingival cell
146 populations supported by known and novel markers.
147

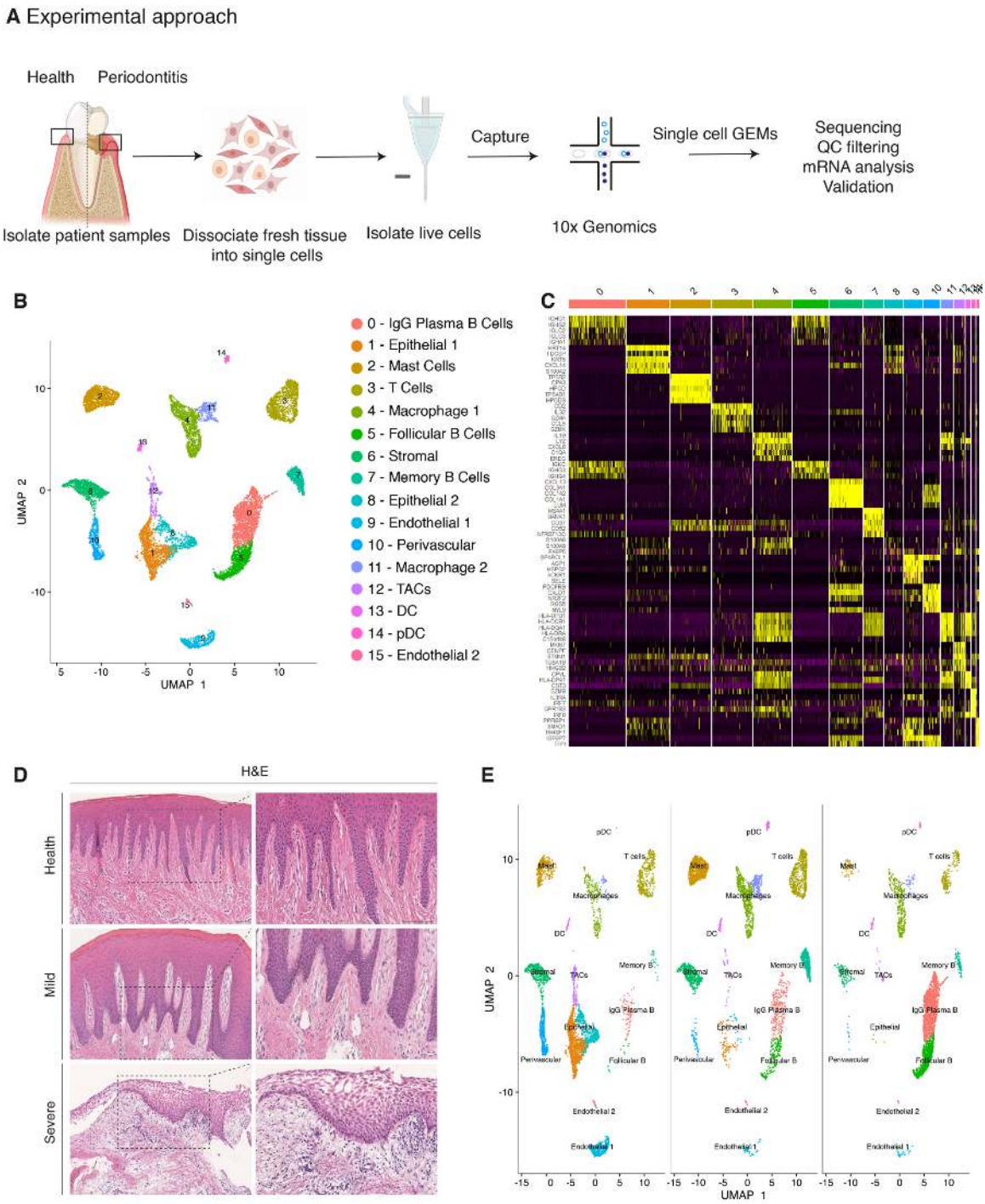

Figure 1. Single-cell Atlas of Gingiva Biopsies from Healthy Individuals and Periodontitis Patients. (A) Overview of the experimental workflow. All samples were processed immediately after clinical surgery. **(B)** scRNA-seq data obtained from healthy and periodontitis cells (n= 12,411) from four donors illustrated by UMAP coloured by cell-type annotation. (**C)** Heatmap of the mean expression of the most differentially expressed marker genes for each cluster identified. **(D)** Haematoxylin and eosin staining of gingival sections from healthy, mild and severe patient samples showing increasing changes in tissue architecture with loss of epithelial rete ridges definition and infiltration of leukocytes. (**E)** Changes in tissue composition in periodontitis showing UMAP of progressive diseased states from healthy, mild, and severely diseased donors.

159 **Transcriptional comparison of healthy and periodontitis reveals progressive**
160 **diseased states**

161 During disease progression there is a distinct signature of clinical phenotypes
162 including redness, swelling, bleeding, destruction of periodontal ligament and bone
163 and gingival recession (Kinane, 2001). These clinical manifestations are due to the
164 dysregulation of a number of cell types which include epithelial, stromal, immune and
165 the associate cross-talk between them. (Pihlstrom et al., 2005).

166 Histologically, the diseased samples showed different levels of severity. Therefore, in
167 our analysis we staged the samples as healthy, mild and severe. (Figure 1D). In the
168 mildly affected sample, we observed an intact keratinised squamous epithelial layer,
169 minor losses of collagen and rete-ridge definition. In contrast, in the severe state we
170 detected a dense infiltrate of lymphocytes, breakdown of the epithelial barrier and clear
171 reduction of collagen content (Figure 1D).

172 To investigate the transitions between health and mild to severe periodontitis, we
173 determined the contribution of cells sampled from each condition to the main cell
174 classes, and investigated whether their respective subpopulations were maintained,
175 amplified or depleted across the conditions.

176 At a transcriptomic level, the cellular landscape is dominated by a corresponding shift
177 in cellular proportions (Figure 1E). In health, we observed low numbers of follicular
178 and plasma B cells and a progressive increase from mild to severe (Figure 1E). The
179 minimal presence of B cells in healthy gingiva was also reported by others (Dutzan et
180 al., 2016, Mahanonda et al., 2016, Artese et al., 2011). Memory B cells show a
181 distinctive increase at disease onset with a subsequent decrease in the severe sample
182 (Figure 1E).

Similarly, there was a surge in T cells in mild disease followed by a decrease in severe. While there has been some characterisation of immune cell subsets in health and periodontitis (Dutzan et al., 2016), the timing of their involvement is still unclear. Our study addresses this to some extent by showing that these populations may be abundant at disease onset and then gradually decrease as disease progresses. T cell senescence as a result of persistent immune activation in chronic diseases has been previously reported (Effros and Pawelec, 1997, Vallejo et al., 2004). A decrease in the severe stage might suggest that the persistent immune activation characteristic of chronic inflammation may lead to T cell senescence, and consequently to the inability to reduce local inflammatory responses contributing to disease persistence. Additionally, we also identified a dynamic shift in the two macrophage populations with an expansion at disease onset consistent with their function in tissue clearing and a subsequent reduction at the severe stage (Figure 1E). There is no clear difference in the dendritic cell compartment during disease progression. Mast cells also show a significant enrichment at disease onset and a decrease in the severe state. These results deliver the first unbiased immune characterisation of the gingiva across disease states (Figure 1E).

In addition to infiltrating immune cells driving the inflammatory process, mesenchymal and epithelial gingival cells in the gingiva are also affected during the progression and persistence of the disease (Yucel-Lindberg and Bage, 2013). We observed a progressive depletion of both mesenchymal and epithelial cell populations (Figure 1E), in line with the patient matched immunohistochemical studies.

Together these results provide with the first comprehensive platform to compare dynamic changes of gingival cell populations during disease development.

Cellular and molecular map of the stromal gingival compartment in health and disease identifies subpopulations with potential roles in disease progression

Tissue mesenchymal cells play essential roles in epithelial homeostasis, matrix remodelling, immunity and inflammation (Kinchen et al., 2018, Nowarski et al., 2017). Their function in the regulation of acute and chronic inflammation in peripheral organs is now well established (Fiocchi et al., 2006, Kinchen et al., 2018, Croft et al., 2019). Despite the growing recognition that the mesenchyme acts as a critical regulator in disease persistence by producing cytokines, chemokines, proteolytic enzymes and prostaglandins (Yucel-Lindberg and Bage, 2013), the identity of gingiva-specific mesenchymal subtypes and the molecular attributes that regulate niche maintenance in disease have not been described. To better visualise the difference in cellular heterogeneity of gingival stromal cells in health and disease, we performed re-clustering analysis of collagen expressing cells to identify any possible sub-clusters with a distinct transcriptional signature.

These data revealed five fibroblast-like populations, one pericyte and one myofibroblast (Figure 2A). Myofibroblasts were identified by expression of *ACTA2* and by gene ontology (GO) terms such as “muscle contraction” and “smooth muscle contraction”. Pericytes were identified by *PDGFRB* and *MCAM* expression and GO terms such as “regulation of angiogenesis” (Figure 2 C, D). S0, S2 and S4 fibroblast-like subpopulations showed enrichment for genes annotated with “extracellular matrix”-related GO terms. Interestingly, one of the fibroblast-like populations (S0) GO enrichment included “upregulation of fibroblast proliferation” with marked expression of *PDGFRA*, *WNT5A* and *IGF1*. It also shows upregulation of *POSTN* which is essential for tissue repair (Kuhn et al., 2007). Another fibroblast-like population (S2) showed enrichment for genes involved in the negative regulation of Wnt signalling

(*GREM1*, *SFRP1*, *APCDD1* and *DKK3*); S4 showed expression of *OSR2*, *FGFR1*, *SOX4* and *TBX3* known to be involved in skeletal development. Additionally, S4 also differed in the expression of a specific form of collagen, collagen IV, which is known to be a key component of the epithelial basement membrane and might suggest a role in epithelial barrier membrane as previously described (Kinchen et al., 2018). Finally, S5 and S6 show a potential role in immune regulation with enrichment for "cytokine-mediated signalling pathway", "IFN-γ signalling" and "T cell activation" (Supplemental Figure 3; Supplemental Table 2). Highly ranked S5 markers included *ILR1*, IFNγR1 and a member of the TNF-receptor superfamily – *TNFRS11B* (osteoprotegerin) which is a negative regulator of bone resorption and thus a key regulator of osteoclast activity (Zaidi, 2007).

To uncover the role of the newly identified mesenchymal subsets in periodontitis, we investigated changes in their contribution across diseased states. Most significantly, we identified a marked decreased in the myofibroblast (S1) and pericyte (S3) subpopulations at disease onset (mild), while the other fibroblast-like cells appeared unchanged with the exception of S6 (Figure 2B). This suggests loss of S1 and S3 cells was the most pronounced change from healthy tissue to mild disease. We further explored the nature of the pro-inflammatory cluster S6 and it included the expression of the major histocompatibility complex (MHC) class II invariant chain (*CD74*) and *AREG* (amphiregulin). Amphiregulin is a reparative cytokine previously described with a role in gingival immune homeostasis (Krishnan et al., 2018). These results identified the potential expansion of a novel stromal population enriched for pro-inflammatory genes in periodontitis.

Next, we investigated whether we could detect these changes using immunofluorescence analysis in gingival tissue samples. We confirmed a progressive

decrease in collagen VI levels suggesting overwhelming changes in the ECM composition and deposition (Figure 2E). We also assessed the myofibroblast and pericyte populations by looking at expression of *ACTA2* and *MCAM* respectively (Figure 2E).

Understanding the pathways underlying stromal differentiation will be essential to understand tissue homeostasis in chronic diseases. Given the lack of markers to reconstruct a cellular trajectory and the knowledge that the number of expressed genes per cells is a hallmark of developmental potential (Teschendorff and Enver, 2017, Han et al., 2020), we used transcriptional diversity to predict candidate stromal precursors (Gulati et al., 2020) (Figure 2F). This analysis placed sub-clusters S5 and S0 as the less differentiated subpopulations, and S1 and S3 (myofibroblasts and pericytes) as fully differentiated states (Figure 3F). Using this pipeline, we identified genes such as *IGHBP4* and *AEBP1* in the less differentiated states.

Overall, we demonstrate that stromal remodelling in periodontitis is heterogenous with a disruption in cell populations known to be involved in tissue repair, and a higher proportion in a pro-inflammatory cell population that could prevent disease resolution. Collectively, these observations suggest that stromal cells shape a permissive inflammatory niche.

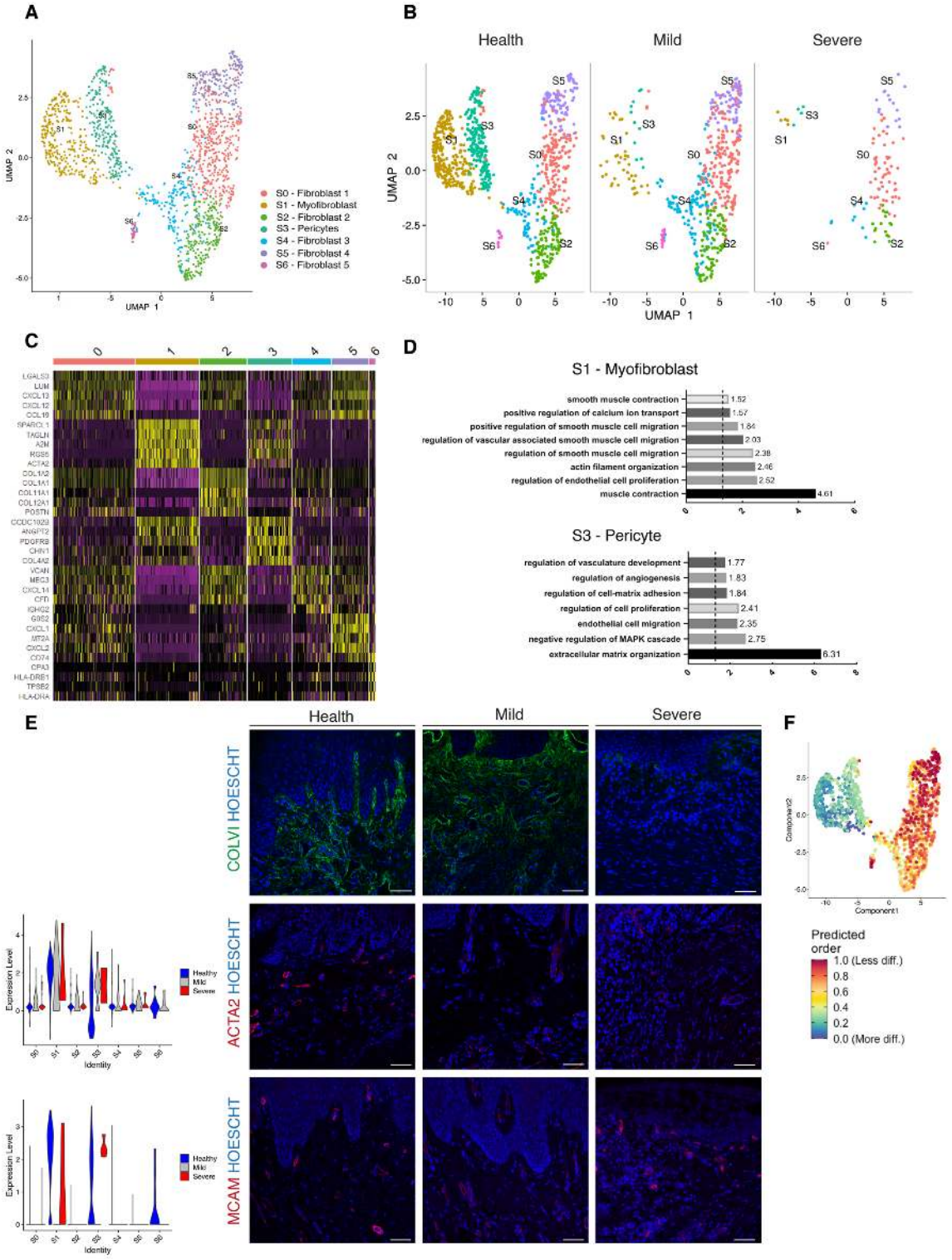

Figure 2. Cellular and molecular map of the stromal gingival compartment in health and disease identifies subpopulations with potential role in disease progression. (**A**) UMAP plot of gingival stromal cells. Single cells coloured by cluster annotation. (**B**) UMAP plot of stromal cells during disease progression. (**C**) Heatmap showing subset-specific markers. (**D**) GO enrichment terms for S1 (myofibroblast) and S3 (pericyte). -log adjusted p-value shown (dotted line corresponds to FDR = 0.05). (**E**) Immunofluorescence staining showing COLVI, ACTA2, MCAM expression throughout disease progression. Scale bars, 100 μm. n= 3 patient samples/condition. Violin plots showing ACTA2 and

MCAM expression across clusters and conditions. (**F)** UMAP annotated with CytoTRACE analysis to predict stromal stem populations. Transcriptional diversity is used here to predict maturation states.

Cellular and molecular map of the epithelial gingival compartment in health and disease

The oral epithelium is one of the fastest renewing tissues in the human body and shows a remarkable regenerative potential. Cell division in epithelial cells takes place in the basal layer which contains the stem cell compartment. After dividing, the committed cells undergo differentiation that leads to expression of structural keratins as cells move superficially (Blanpain and Fuchs, 2009). Recent work has started to elucidate epithelial heterogeneity in the basal layer using mouse models (Jones et al., 2019, Byrd et al., 2019). However, little is known about human gingival epithelial cell heterogeneity and its role in disease. Thus, we further explored the single-cell transcriptomes of epithelial clusters (1, 8 and 12).

By re-clustering the epithelial cells, we identified ten populations (Figure 3A). Two basal cell populations were identified in E0 and E1. E0 shows expression of *HOPX* which marks known stem cells in the intestinal and skin epithelia (Takeda et al., 2013, Takeda et al., 2011) and *IGFBP5* which is enriched in transit-amplifying cells (TACs) in the interfollicular epidermis (Tumbar et al., 2004) and recently shown through lineage-tracing to label oral epithelial stem cells in the hard palate (Byrd et al., 2019). E1 indicated a more mature basal cell state with expression of *DDR1* known as a cell surface receptor for fibrillar collagen, and *COL17A1*. Cycling basal cells were identified in E5 by expression of *MKI67* and *AURKB*. E2 showed enrichment for *SAA1* and *TNFRSF21* both involved in chronic inflammatory conditions. E3 showed enrichment for B cell receptor signalling pathway, and E4 and E8 for neutrophil mediated immunity. We further identified E6 and E7 with a role in cell cycle regulation. Finally, E9 had a gene expression profile consistent with a role in ECM organisation and angiogenesis (Figure 3A, D; Figure S4).

Next, we investigated changes in epithelial cell composition and gene expression through the different disease states (Figure 3B). At disease onset (mild), we observed a depletion in E6 and E7 populations which show enrichment in genes involved in cell cycle regulation; and in E9 which is involved in ECM organisation. Cycling cells (E5) show a decrease in mild, and a subsequent increase in severe (Figure 3B). We detected an increase in E8 defined in GO terms by “cytokine mediated signalling” (Figure 3 B, D). Next, we asked which epithelial signals are predicted to modulate the identified stem cell signature found in E0 in disease. Using NicheNet (Browaeys et al., 2020) we identified sub-cluster E8 as the main signalling source predicted to modulate E0 through the expression of several ligands including *MMP9*, *SPN* and *HLA-DRA* (Figure 3E). While more work is necessary to understand the functional role of the E8 subpopulation, targeting this subpopulation in future immune-modulatory experiments may lead to important findings.

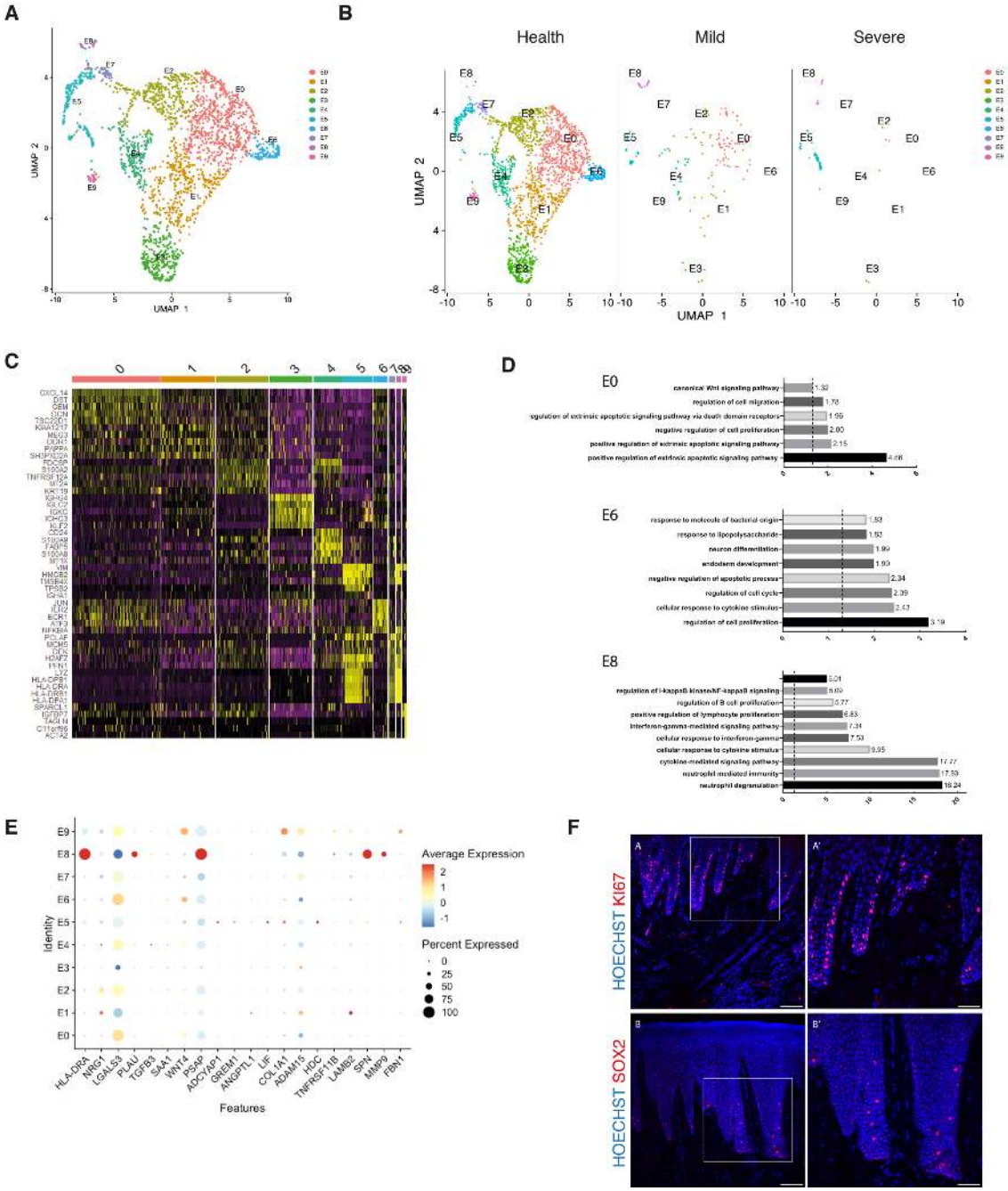

Figure 3. Cellular and molecular map of the epithelial gingival compartment in health and disease. (**A)** UMAP plot of human gingival epithelial cells. Single cells coloured by cluster annotation. (**B)** UMAP plot of epithelial cells during disease progression. (**C)** Heatmap showing subset-specific markers. (**D)** GO enrichment terms for E0, E6 and E8 with -log adjusted p-value shown (dotted line corresponds to FDR = 0.05). (**E)** Dot plot showing top predicted ligands expressed by epithelial cells that modulate the E0 (stem) compartment. (**F)** Expression of KI67 and SOX2 in human healthy tissue. KI67 marks proliferative cells (cluster E5), and SOX2 marks an epithelial stem cell compartment (cluster E0). Scale bars = 100 μm (A, B). Scale bars, 50 μm (A', B'). n = 4 patient samples/condition.

Identifying ligand-receptor interactions and transcriptional regulation contributing to disease progression

Periodontitis is characterised by tissue remodelling, which depends on complex interactions between stromal, epithelial and immune cells. However, how these cells interact to contribute to tissue homeostasis and how these interactions are dysregulated during disease remains poorly defined. To understand this cross-talk, we used NicheNet (Browaeys et al., 2020) to model which cellular signals induce a stromal and perivascular response in periodontitis (Figure 4A).

In healthy and mild stages, the cell-stromal/cell-perivascular interaction landscape was dominated by endothelial, stromal, macrophage and epithelial originating signals (Figure 4B). As disease progresses, in mild and severe stages, we observed a clear loss in endothelial and stromal originating signals, and an increase in macrophage, mast, T and B cell signalling (Figure 4B). Analysis of these cell-cell interactions revealed several signalling pathways including tumour necrosis factor (TNF) and bone morphogenetic protein (BMP) signalling (Figure 4B). Overall, the number of predicted interactions in severe disease was strongly reduced.

We next focused on epithelial-mesenchymal interactions in the mild stage by investigating which signalling interactions could potentially induce an inflammatory signature in the mesenchymal compartment (Figure 4C). Analysis of epithelial ligands predicted to cause an inflammatory response revealed *IL1*, *EDN1*, *TNF*, *LTB* and *BMP2* as the main contributors to the mild inflammatory stage (Figure 4D). Proliferative cells (TACs) are suggested to be the main source of these ligands with the exception of *BMP2* (Figure 4D). We next analysed which stromal and perivascular receptors can potentially bind to these identified epithelial ligands (Figure 4E) and the target genes of these ligand-receptor interactions (Figure 4F). We estimated

prominent *IL1B-CXCL9*, *TNF-CXCL9*, *TNF-UBD*, *BMP2-COL1A2* interactions, suggesting that these molecular interactions may be crucial in sustaining a proinflammatory microenvironment. Target genes were confirmed to be differentially expressed with disease (Figure 4G). *IL1B* and *TNF* epithelial ligands specifically targeted S0 and S5 stromal subpopulations, and *BMP2* all fibroblast-like subpopulations and pericytes (Figure 4H).

Together, these results identify *IL1B*, *EDN1*, *TNF* and *BMP2* as the main epithelial modulators driving an inflammatory response in stromal and perivascular cells. Based on their expression, we identified novel epithelial-mesenchymal interactions in periodontitis: the interactions between epithelial *IL1B* and *TNF* and stromal target genes.

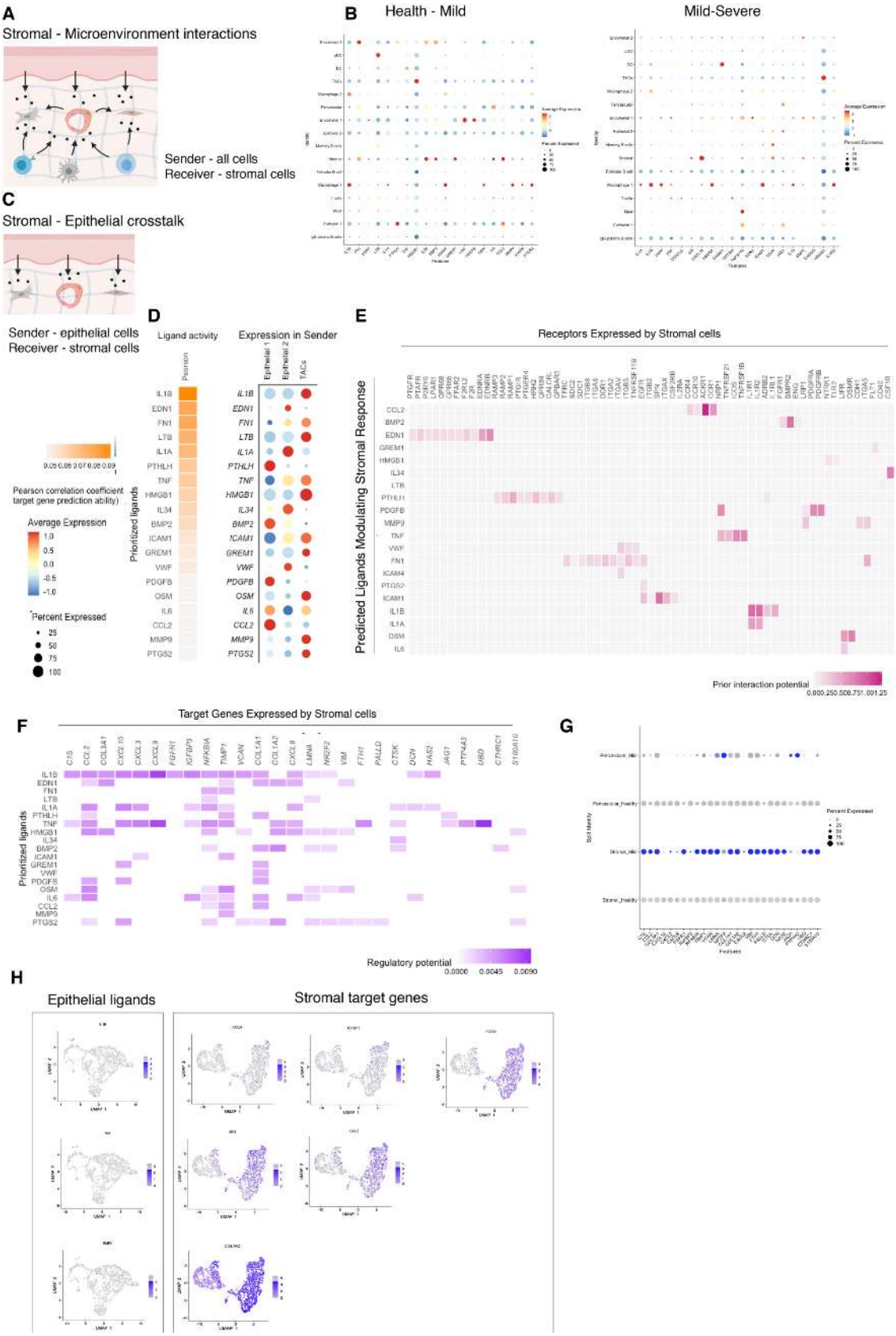

411

412 **Figure 4. Unbiased cell-cell interaction analysis and its effect in the stromal microenvironment.**
413 (**A)** Schematic representation of the NicheNet analysis of upstream ligand-receptor pairs and stromal
414 target genes inducing DE genes in periodontitis. Created with BioRender.com. (**B)** Dot plots depicting
415 which gingival cell populations express top-ranked ligands contributing to the transcriptional response

observed from health to mild disease and from mild to severe in the stromal compartment. (**C)** Schematic representation of the NicheNet analysis of epithelial-mesenchymal crosstalk in mild disease. Created with BioRender.com. (**D)** Top predicted epithelial ligands driving the stromal inflammatory response and dot plot showing which epithelial subpopulation express these ligands. (**E)** Ligand-receptor heatmap of potential receptors expressed by stromal cells associated with each epithelial ligand. (**F)** Ligand-target heatmap of stromal and perivascular target genes of the identified epithelial ligands. (**G)** Dot plot confirming upregulation of the identified stromal target genes in disease. (**H)** UMAPs feature plots mapping the identified epithelial ligands and target genes to the respective target genes expressed by stromal cells.

Single-cell transcriptomics of human B cells reveals activation signature in periodontitis

B cells are essential in the generation of protective immunity. However, tissue-based B cell subsets are not well characterised in human oral tissues. Following our observations that there is a consistent increase of B cells in line with disease severity, and their established role in disease immunopathogenesis, we next focused on the humoral response by performing a more in-depth transcriptomic analysis. Previous studies have established that B cells constitute the majority of cells in periodontitis lesions (Thorbert-Mros et al., 2015), and it has been suggested a dual protective and detrimental role (Oliver-Bell et al., 2015, Abe et al., 2015).

We compared their transcriptional profiles across disease states (Figure 5A). We found a profound prevalence of IgG plasma B cells in disease which is supported by another study (Kinane et al., 1999) in periodontitis patients. Similarly, it has been reported an increase in local IgG within the gastrointestinal tract during intestinal inflammation (Castro-Dopico et al., 2019). Here, we found IgG plasma cells almost absent in health and distinctively expanded with disease progression (Figure 5A). Upregulation of an *IGH* signature has been previously linked to disease severity and renders activation of the mononuclear phagocyte response in the intestinal mucosa (Castro-Dopico et al., 2019). In humans, mucosal IgG responses are pro-inflammatory when they involve complement activation. This cluster showed enrichment of genes involved in the complement system such as CFB and C2 (Figure 5D). This system plays a critical role in signalling B cell activation (Carroll and Isenman, 2012, Chen et al., 2020), and previous research has established a role in periodontitis.

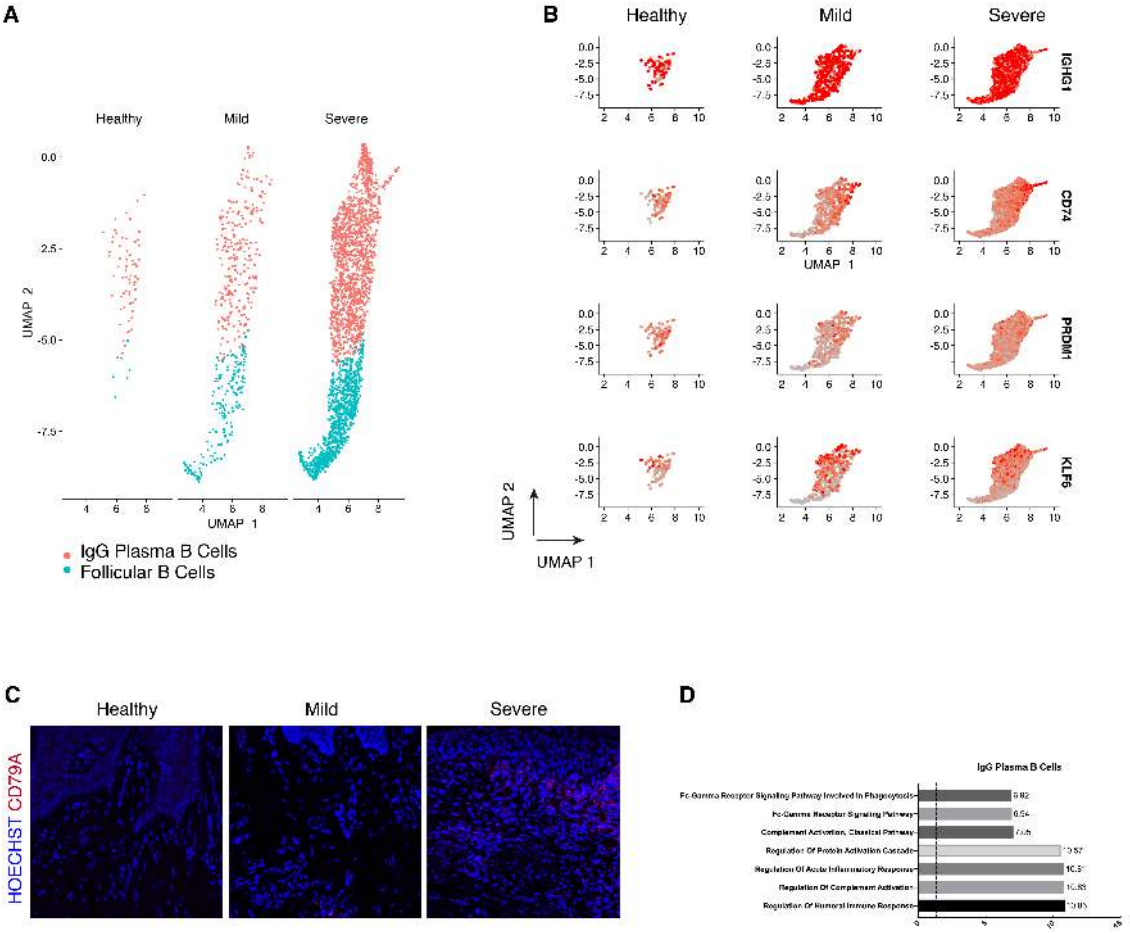

Figure 5. Periodontitis induces an IgG plasma B cell signature in human gingiva. (A) UMAP analysis of human B cells identifying follicular and IgG plasma B cells split by condition. (**B)** UMAP expression plots of human B cell subset markers. Cells coloured by normalised expression of indicated genes. (**C)** CD79A in human gingival tissue across health and disease. Scale bars, 100 μm. n = 3 patient samples/condition. (**D)** Gene enrichment analysis of IgG Plasma B cells. -log adjusted p-value shown (dotted line corresponds to FDR = 0.05).

Discussion

The human gingiva is a unique barrier site since failure to appropriately control immune responses leads to periodontitis. However, the molecular mechanisms of homeostasis and how they are disrupted in disease are poorly understood. Previous studies have reported on gene expression in gingival tissue from patients with periodontitis, however these studies have used conventional bulk RNA sequencing on whole-biopsies which average gene expression changes across the whole tissue, and therefore lose all information of discreet cellular subpopulations (Becker et al., 2014, Davanian et al., 2012, Demmer et al., 2008, Kim et al., 2016, Lundmark et al., 2015). In this work, we provided the first comprehensive cellular landscape of *in vivo* human gingiva, charting dynamic cellular composition differences at single-cell level across disease states. Our atlas comprises all the main gingival cell types defined by the expression of canonical and novel gene markers, with highly consistent results across all samples tested. Next, we analysed the potential molecular signals driving the inflammatory response in the stromal niche.

We identified a striking difference in mesenchymal and epithelial cells during disease progression. In the mesenchymal lineage, we identified populations of established cells, such as myofibroblasts and pericytes, and five additional distinct populations of fibroblast-like cells. Recent studies have started to elucidate the role of stromal cell populations in tissue homeostasis (Shoshkes-Carmel et al., 2018, Bahar Halpern et al., 2020, Greicius et al., 2018), and consistent with previous studies we identified two populations expressing Wnts and Wnt inhibitors suggesting the presence of mesenchymal niche regulating populations (Kinchen et al., 2018, Kim et al., 2020) that may be required for oral mucosa maintenance. In periodontitis, we observed that these populations were preserved in the mild stage, whereas the myofibroblast and pericyte

populations were strikingly reduced. Myofibroblasts are known to be responsible for excessive synthesis, deposition and remodelling or extracellular matrix proteins (Tomasek et al., 2002), however less is known about the mechanisms that promote their survival and persistence in inflammatory conditions. Multiple single-cell analysis have revealed that myofibroblast populations are heterogenous and undergo dynamic changes during tissue repair in various organs (Farbehi et al., 2019, Guerrero-Juarez et al., 2019, Xie et al., 2018, Tabib et al., 2018, Peyser et al., 2019, Lambrechts et al., 2018). Our observation that myofibroblasts are reduced in the transition from health to mild disease, might suggest a contribution to ECM degradation and to the state of chronic inflammation characteristic of periodontitis. Previous research has suggested two mechanisms that limit myofibroblast survival; either a dependence on growth factor receptor-mediated pathways required for their survival (Bostrom et al., 1996), or pro-apoptotic cytokines might selectively induce apoptosis by directly activating cell death signalling pathways or by inhibiting pro-survival pathways. One example is IL-1B which induces caspase-dependent apoptosis in mouse lung myofibroblasts by inhibiting FAK (Zhang and Phan, 1999). We also detected a decrease in the pericyte population from health to mild disease. Pericytes are present in all vascularised tissues, and provide structural support to the vasculature with proven roles in angiogenesis (Lindblom et al., 2003), wound healing (Kramann et al., 2015), progenitor cell functions (Crisan et al., 2008) and immunomodulation (Meyers et al., 2018). It has been demonstrated that there is an expansion and dilation of the vasculature in periodontitis (Zoellner et al., 2002), contributing to increased leukocyte recruitment into the tissue. The loss or detachment of pericytes has been implicated in disease (Armulik et al., 2011), and has been related to infiltration of inflammatory cells (Ogura et al., 2017). Interestingly, *Pdgfb* or *Pdgfr* loss-of-function embryos show

vascular hyperplasia and microvessel dilation (Hellstrom et al., 2001). We hypothesise that the observed pericyte decrease might impair the stromal compartments ability to regenerate as these are mesenchymal stem cell precursors *in vivo* (Sacchetti et al., 2016, Yianni and Sharpe, 2018).

In periodontitis, we observed the emergence of one fibroblast-like population highly enriched in pro-inflammatory genes such as AREG. Overall, we observed stromal remodelling in a subpopulation specific way and in accordance with previous reports (Kinchen et al., 2018). Normal repair and regeneration responses are compromised, while continuous production of pro-inflammatory factors prevent inflammatory resolution.

This work also provides the first comprehensive analysis of the human gingival epithelium. Understanding the molecular mechanisms underlying this mucosal barrier can help shape immunoregulatory responses in the context of homeostasis and disease. Our data identified a basal progenitor cell population expressing *HOPX* and *IGFBP5*. Although, recent studies have started to elucidate oral progenitor cells' heterogeneity, this is the first human detailed characterisation that will allow the development of future validation models. We identified one epithelial subpopulation (E8) expanded in disease, and intercellular communication analysis suggested that this population is the main signalling centre driving the epithelial inflammatory response. More work is needed to address this finding and the immunoregulation of this population.

We provided an extensive immune repertoire profiling and described in detail the expansion of B cell subtypes. These results are consistent with data obtained in a previous study despite the difference in tissue collection. Our samples were obtained from sites which had received non-surgical treatment but still had residual disease and

561 the Dutzan study collected from a cohort that had never been treated for disease
562 (Dutzan et al., 2016). We also observed a T cell-rich inflammatory infiltrate with
563 minimal B cells present in health. This rich and diverse immune network present in
564 health explains the immunosurveillance required to control the constant bacterial
565 exposure. Dutzan *et al*, identified neutrophils as the most notable cellular difference in
566 periodontitis. In our FACS gating strategy, neutrophils co-localised extensively with
567 debris and were therefore excluded to avoid contamination.
568 We specifically provided a detailed molecular description of B cell subsets as it was
569 the major cellular shift detected in the immune cell network. This is consistent with
570 previous observations showing that the most upregulated genes in periodontitis are
571 involved in B cell development (Lundmark et al., 2018). Despite the knowledge that
572 atypical activation of B cells contribute to disease progression by their antigen-
573 presentation, cytokine production, and expression and secretion of receptor activator
574 of nuclear factor-kB ligand (RANKL), contributing to osteoclastogenesis (Thorbert-
575 Mros et al., 2015), little is known about the molecular mechanisms driving these
576 processes. We identified a specific IgG plasma cell response. Recently, a IgG
577 contribution has been specifically linked with driving chronic inflammatory responses
578 (Castro-Dopico et al., 2019). In that study, patient samples with higher levels of IgG
579 has the highest disease severity scores and correlated with neutrophil infiltration and
580 IL-1B expression. In our study, this response was associated with complement
581 activation. Previously, complement split products were found absent or present at low
582 concentrations in healthy individuals, but abundant in periodontitis (Damgaard et al.,
583 2015, Hajishengallis et al., 2017). Continuous complement activation promotes
584 survival of local pathogens in a nutritionally favourable inflammatory environment that
585 promotes dysbiosis and disease development (Hajishengallis et al., 2017,

586 Hajishengallis et al., 2011, Maekawa et al., 2014). Our findings have therapeutic
587 implications by identifying IgG signalling as a potential therapeutic target in
588 periodontitis.
589 Finally, we aimed to identify the signals driving the inflammatory response in the
590 stromal compartment. Previous studies have reported IL1B and TNF as key regulators
591 in the periodontitis pathogenesis (Yucel-Lindberg and Bage, 2013), therefore it was
592 not surprising to find these molecules highly represented in our cell interaction analysis
593 (Figure 6). We described newly identified molecular mechanisms involved in the
594 regulation of these cytokines by predicting new receptor interactions and previously
595 unidentified target genes. These findings bring new perspectives on periodontitis
596 molecular mechanisms governing tissue loss and future experiments will be important
597 to test these predictions.
598 In summary, we have established the first human gingiva cell atlas, revealing
599 heterogeneity within major gingiva cell populations and providing with a roadmap for
600 further functional insights into the immune and structural populations present in the
601 gingiva. It also provides new biological insights into the immunopathogenesis of
602 periodontitis. These data offer enormous potential for medicine, drug discovery and
603 diagnostics through a more detailed understanding of cell types, basic biological
604 processes and disease states.
605
606
607
608
609
610

Materials and Methods

Patient recruitment and ethical approval

Human gingival samples were obtained from consenting patients undergoing routine periodontal surgical procedures (Department of Periodontology, Guy's Hospital, King's College London). All samples were collected and processed in compliance with the UK Human Tissue Act (Human Tissue Authority #203019), ethically approved by the UK National Research Ethics Service (Research Ethics Committee 17/LO/1188). Written informed consent was received from participants prior to inclusion in the study. Cohort inclusion criteria for all subjects were: absent history of relevant medical conditions, no use of medication, no use of nicotine or nicotine-replacement medications, no pregnancy and breast feeding.

Healthy controls included crown lengthening procedures, and periodontitis patients, pocket reduction surgeries. Patients with periodontitis had tooth sites with probing depth $\geq$ 6 mm, and bleeding on probing. Patients used as controls showed no signs of periodontal disease, with no gingival/periodontal inflammation, a probing depth $\leq$ 3 mm, and no bleeding on probing.

Patient 33. Gender: male. Age band: 41-65. No history of periodontal disease. Site: buccal gingival margin.

Patient 35. Gender: female. Age band: 41-65. Chronic periodontitis with previous history of non-surgical treatment. Site: buccal gingival margin.

Patient 37. Gender: male. Age band: 41-65. Chronic periodontitis with previous history of non-surgical treatment. Site: buccal gingival margin.

Patient 38. Gender: male. Age band: 41-65. No history of periodontal disease. Site: buccal gingival margin.

Histology and Microscopy

Human gingival tissue was freshly collected and fixed overnight in 4% neutral buffered formalin. Then, tissue underwent three 5-minute washes in PBS at room temperature followed by dehydration washes in increasing ethanol concentrations. After dehydration, tissue was processed using a Leica ASP300 Tissue Processing for one hour. Tissues were then embedded in paraffin. Serial sections (12 µm thick) were cut for haematoxylin and eosin (H&E) and immunohistochemistry (IHC) staining.

H&E was carried out for each patient sample using an Automated Slide Stainer. Slides were dewaxed by immersion in Neo-Clear® (Merck Millipore), twice for 10 minutes. Tissue was then rehydrated by decreasing volumes of ethanol in deionised H_20 (100%, 90%, 70%, 50%) for two minutes in each step and rinsed in deionised H_20 for 2 minutes. Samples were then stained in Ehrlich's Haematoxylin (Solmedia) for 10 minutes followed by a 10-minute rinse under running water and then a two-minute rinse in deionised H_20. Tissue was then stained in 0.5% Eosin Y (Sigma-Aldrich) for 5 minutes and washed twice in deionised H_20. Samples were dehydrated in increasing IMS in deionised H_20 concentration steps (70%, 90%, 100%, 100%) for two minutes each. Slides were immersed in Neo-Clear® three times for 5 minutes and then mounted using Neo-mount® mounting medium (Merck Millipore), coverslipped and left to dry overnight in at 42°C.

Immunohistochemical staining

Immunofluorescence staining was performed on 12 µm sections as described above. In short, slides were dewaxed in Neo-Clear twice for 10 minutes and rehydrated in a series of decreasing ethanol volumes as described above. Heat induced epitope retrieval was performed with sodium citrate buffer (pH 6) in a Decloaking chamber NXGEN (Menarini Diagnostics) for 3 minutes at 110°C. Slides were cooled to room

temperature before blocking for 1 hour at room temperature in Blocking Buffer (0.2% BSA, 0.15% glycine, 0.1% TritonX in PBS) with 10% goat or donkey serum depending on the secondary antibody used. Primary antibodies were diluted in blocking buffer with 1% of the respective blocking buffer and incubated overnight at 4°C. The following day, slides were washed three times in PBST and incubated with the respective secondary antibodies diluted 1:500 in 1% blocking buffer for one hour at room temperature. Slides were mounted with Citifluor™ AF1 mountant media (Citifluor Ltd., AF1-100) and cover slipped for microscopy. Slides were put to dry in a dry chamber that omitted all light, and kept at 4°C.

The following antibodies were used: COLVI raised in rabbit (ab182744, 1:500, Alexa Fluor-488 secondary), ACTA2 raised in mouse (ab7817, 1:200, Alexa Fluor-633), MCAM raised in rabbit (ab75769), (KI-67 raised in rabbit (ab5580, 1:100, Alexa Fluor-594), SOX2 raised in rabbit (ab92494, 1:100, biotinylated secondary), CD79A raised in rabbit (ab79414, 1:100, Alexa Fluor -488 secondary).

Imaging

For bright field images, stained slides were scanned with Nanozoomer-XR Digital slide scanner (Hamamatsu) and images processed using Nanozoomer Digital Pathology View. Fluorescent staining was imaged with a TCS SP5 confocal microscope (Leica Microsystems) and Leica Application Suite Advanced Fluorescence (LAS-AF) software. Images were collected and labelled using Adobe Photoshop 21.1.2 software and processed using Fiji (Schindelin et al., 2012).

Tissue processing for single cell isolation

Fresh tissues were processed immediately after clinical surgery using the same protocol. Tissue was transferred to a sterile petri dish and cut into <1mm^3 segments before being transferred to a 15 mL conical tube. Tissue was digested for 30 minutes

686 at 37ºC with intermittent shaking using an enzymes dissociation kit (Miltenyi, Bergisch-
687 Gladbach, Germany). The resulting cell suspension was filtered through a 70-µm cell
688 strainer to ensure a single cell preparation and cells collected by centrifugation (1,200
689 rpm for 5 minutes at 4°C). Cells were resuspended in 0.04% non-acetylated BSA
690 (UltraPure™ BSA, ThermoFisher Scientific) and stained with 1.5 µg DAPI (D1306,
691 Invitrogen) used as dead cell exclusion marker. Samples were analysed on BD FACD
692 Aria III fusion machine. Cells were gated based on size using standard SSC-A and
693 FSC-A parameters so that debris is excluded. Doublets were excluded using SSC-A
694 and SSC-W parameters. Live cells were selected as cells identified to be dimly
695 fluorescing in DAPI and were then sorted into chilled FACS tubes prefilled with 0.04%
696 300µl BSA. Single cell suspensions were captured using the 10X Genomics®
697 Chromium Single Cell 3' Solution (v3) according to the manufacturers protocol. Cells
698 were resuspended separately in PBS with 0.04% BSA at a density of 50-100 cells per
699 µL.

700 **Chromium 10x Genomics library and sequencing**

701 Single-cell suspensions were manually counted using a haemocytometer and
702 concentration adjusted to a minimum of 300 cells μL^{-1}. Cells were loaded according to
703 standard protocol of the Chromium single-cell 3' kit to capture around 5,000 cells per
704 chip position. Briefly, a single-cell suspension in PBS 0.04% BSA was mixed with RT-
705 PCR master mix and loaded together with Single Cell 3' Gel Beads and Partitioning
706 Oil into a Single Cell 3' Chip (10x Genomics) according to the manufacturer's
707 instructions. RNA transcripts from single cells were uniquely barcoded and reverse
708 transcribed. Samples were run on individual lanes of the Illumina HiSeq 2500.

709

710

Computational analysis of sc-RNAseq datasets

The cell ranger pipeline was used for processing of the single-cell RNAseq data files prior to analysis according to the instructions provided by 10x Genomics. Briefly, base call files obtained from each of the HiSeq2500 flow cells used were demultiplexed by calling the 'cellranger mkfastq'. Resulting FASTQ files were aligned to the human reference genome GRCh37/hg19 and subsequently filtered and had barcodes and unique molecular identifiers counted and count files generated for each sample. These were used for subsequent processing and data analysis using R.

Integrative analysis

Integrated analysis was performed according to the authors of the Seurat package (Butler et al., 2018, Stuart et al., 2019). Briefly, count files for each condition were read into RStudio and cells corresponding to each condition were labelled accordingly as 'Healthy', 'Mild' and 'Severe'. Only cells found to be expressing more than 500 transcripts were considered as to limit contamination from dead or dying cells. Each dataset was normalised for sequencing depth by calling the 'NormalizeData' function and the 2000 most variable features of each dataset were detected using the "vst" method by calling the 'FindVariableFeatures' function. Subsequently the 'FindIntegrationAnchors' function was called to identify anchors across the datasets and the 'IntegrateData' function to integrate them so an integrated analysis could be run on all cells simultaneously. The data was then scaled to account for sequencing depth using 'ScaleData' and PCA components were used for an initial clustering of the cells (using 'RunPCA'). 20 dimensions were used to capture the majority of the variability across the datasets. 'FindNeighbors' was then used, utilising the above dimensionality parameters to construct a K-nearest neighbour graph based on Euclidian distances in PCA space. The clusters are then refined by applying a Louvain

algorithm that optimises the modularity of the dataset and groups the cells together based on global and local characteristics. This is done by calling the 'FindClusters' function. We then run non-linear dimensionality reduction using UMAP to be able to visualise and explore the datasets. The same principle components were used as above. The Stromal, Epithelial and B-cell clusters were then extracted using the 'Subset' function.

Stromal cell re-clustering analysis

Stromal clusters were identified as being 'collagen producing'. These two clusters were reanalysed separately from the integrated dataset. Stromal cells were filtered to only utilise live cells using percentage of mitochondrial gene expression as an exclusion metric (<15%). Datasets were then re-normalised by calling the 'NormalizeData' function to account for the reduction in cell numbers subsequent to subseting the data. According to the author instructions, the top 2000 most variable features across the dataset were then identified using the 'FindVariableFeatures'. These variable features were subsequently used to inform clustering by passing them into the 'RunPCA' command. Using 'Elbowplot' we identified that the first 8 principle components should be used for downstream clustering when invoking the 'FindNeighbors' and 'RunUMAP', as detailed above.

Epithelial cell re-clustering

Epithelial cells were identified from the epithelial clusters in the integrated UMAP and re-clustered as explained above with some minor exceptions. Epithelial cells were isolated as being the clusters 1, 8, 12. The first 5 principal components were used as these were identified as being significant by the 'Elbowplot' function.

Gene Ontology (GO) analysis

Gene ontology (GO) analysis was performed using Enrichr (Chen et al., 2013) on the top 200 differentially expressed genes (adjusted p value < 0.05 by Wilcoxon Rank Sum test). GO terms shown are enriched at FDR < 0.05.

CytoTRACE

An expression matrix consisting of only the specified sub-set of cellular populations was used as a starting point. CytoTRACE analysis was performed according to the developer's instructions (Gulati et al., 2020). The resulting embeddings were then projected onto the UMAP projections.

NicheNet analysis

This analysis predicts which ligands produced by a sender cell regulate the expression of receptors/target genes in another (receiver) cell. We followed the open source R implementation available at GitHub (https://github.com/saeyslab/nichenetr). For differential expression we used FindMarkers function in Seurat to generate average logFC values per cell type. For Figure 3E, we assigned all epithelial populations as 'sender cells' and E0 as 'receiver' to derive a set of predicted epithelial ligands modulating the mild response seen in this specific subpopulation. For Figure 4B, we assigned all cell types as 'sender cells' and the stromal populations as 'receiver' and extracted all cell type signatures by taking the 100 differentially expressed genes isolated in health/mild and in mild/severe.

For Figure 4D-G, we defined all epithelial populations as 'sender' and all stromal as 'receiver' in health vs mild responses.

Data availability

Raw sequencing data obtained from patients used in this study is deposited under GSE152042. These will become available upon acceptance of the manuscript.

Study approval

Informed consent in writing before their participation in this study was obtained from each subject in compliance with the UK Human Tissue Act (Human Tissue Authority #203019), and ethically approved by the UK National Research Ethics Service (Research Ethics Committee 17/LO/1188).

Author contributions

A.J.C contributed to conception, design, ethical approval, patient informed consent, sample processing, wet laboratory experiments, bioinformatic analysis, data analysis and interpretation, drafted and critically revised the manuscript; V. Y performed bioinformatic analysis, interpretation of data, drafted and critically revised the manuscript; A.A.V contributed to conception, design, ethical approval and critically revised the manuscript; V. B contributed to conception, design, ethical approval, patient informed consent and sample collection; E.D'A contributed to conception, design and critically revised the manuscript; P.T.S acquired funding, contributed to conception, design, data analysis and interpretation, drafted and critically revised the manuscript. All authors gave final approval and agree to be accountable for all aspects of the work.

Acknowledgements

We thank all the patients who contributed to this study, the support of our Periodontology MClinDent students, GSTT nursing staff and Dr Pegah Heidarzadeh Pasha at Guy's Hospital. We thank all CCRB laboratory technicians for their support, especially Dr Alasdair Edgar for tissue processing and H&E staining, and Dr Susmitha Rao for tissue culture. We acknowledge support of the BRC Flow Cytometry and BRC Genomics cores at Guy's Hospital for their services. We thank Dr Ranjit Bhogal, Dr Fei Ling Lim, Miss Alison Russell and Dr Jenny Pople for their support at Unilever. The research described was supported by the BBSRC Industrial CASE Studentship (Grant Ref: BB/P504506/1) and National Institute for Health Research's Biomedical Research Centre based at Guy's and St Thomas' NHS Foundation Trust and King's College London. The views expressed are those of the authors and not necessarily those of the NHS, the National Institute for Health Research, or the Department of Health. This work was funded by Unilever in the form of a research grant awarded to P.T.S .

The authors state no conflict of interest. However, for the record, ED'A is an employee of Unilever Plc.

References

ABE, T., ALSARHAN, M., BENAKANAKERE, M. R., MAEKAWA, T., KINANE, D. F., CANCRO, M. P., KOROSTOFF, J. M. & HAJISHENGALLIS, G. 2015. The B Cell-Stimulatory Cytokines BLyS and APRIL Are Elevated in Human Periodontitis and Are Required for B Cell-Dependent Bone Loss in Experimental Murine Periodontitis. *J Immunol,* 195**,** 1427-35. DOI: 10.4049/jimmunol.1500496

ABRAHAM, S. N. & ST JOHN, A. L. 2010. Mast cell-orchestrated immunity to pathogens. *Nat Rev Immunol,* 10**,** 440-52. DOI: 10.1038/nri2782

AKKAYA, M., KWAK, K. & PIERCE, S. K. 2020. B cell memory: building two walls of protection against pathogens. *Nat Rev Immunol,* 20**,** 229-238. DOI: 10.1038/s41577-019-0244-2

ARMULIK, A., GENOVE, G. & BETSHOLTZ, C. 2011. Pericytes: developmental, physiological, and pathological perspectives, problems, and promises. *Dev Cell,* 21**,** 193-215.DOI: 10.1016/j.devcel.2011.07.001

ARTESE, L., SIMON, M. J., PIATTELLI, A., FERRARI, D. S., CARDOSO, L. A., FAVERI, M., ONUMA, T., PICCIRILLI, M., PERROTTI, V. & SHIBLI, J. A. 2011. Immunohistochemical analysis of inflammatory infiltrate in aggressive and chronic periodontitis: a comparative study. *Clin Oral Investig,* 15**,** 233-40. DOI: 10.1007/s00784-009-0374-1

BAHAR HALPERN, K., MASSALHA, H., ZWICK, R. K., MOOR, A. E., CASTILLO-AZOFEIFA, D., ROZENBERG, M., FARACK, L., EGOZI, A., MILLER, D. R., AVERBUKH, I., HARNIK, Y., WEINBERG-COREM, N., DE SAUVAGE, F. J., AMIT, I., KLEIN, O. D., SHOSHKES-CARMEL, M. & ITZKOVITZ, S. 2020. Lgr5+ telocytes are a signaling source at the intestinal villus tip. *Nat Commun,* 11**,** 1936.DOI: 10.1038/s41467-020-15714-x

BECKER, S. T., BECK-BROICHSITTER, B. E., GRAETZ, C., DORFER, C. E., WILTFANG, J. & HASLER, R. 2014. Peri-implantitis versus periodontitis: functional differences indicated by transcriptome profiling. *Clin Implant Dent Relat Res,* 16**,** 401-11.DOI: 10.1111/cid.12001

BERNARDO, M. E. & FIBBE, W. E. 2013. Mesenchymal stromal cells: sensors and switchers of inflammation. *Cell Stem Cell,* 13**,** 392-402.DOI: 10.1016/j.stem.2013.09.006

BLANPAIN, C. & FUCHS, E. 2009. Epidermal homeostasis: a balancing act of stem cells in the skin. *Nat Rev Mol Cell Biol,* 10**,** 207-17.DOI: 10.1038/nrm2636

BOSTROM, H., WILLETTS, K., PEKNY, M., LEVEEN, P., LINDAHL, P., HEDSTRAND, H., PEKNA, M., HELLSTROM, M., GEBRE-MEDHIN, S., SCHALLING, M., NILSSON, M., KURLAND, S., TORNELL, J., HEATH, J. K. & BETSHOLTZ, C. 1996. PDGF-A signaling is a critical event in lung alveolar myofibroblast development and alveogenesis. *Cell,* 85**,** 863-73.DOI: 10.1016/s0092-8674(00)81270-2

907 BROWAEYS, R., SAELENS, W. & SAEYS, Y. 2020. NicheNet: modeling intercellular
908 communication by linking ligands to target genes. *Nat Methods,* 17**,** 159-162.DOI:
909 10.1038/s41592-019-0667-5
910
911 BUTLER, A., HOFFMAN, P., SMIBERT, P., PAPALEXI, E. & SATIJA, R. 2018.
912 Integrating single-cell transcriptomic data across different conditions, technologies, and
913 species. *Nat Biotechnol,* 36**,** 411-420.DOI: 10.1038/nbt.4096
914
915 BYRD, K. M., PIEHL, N. C., PATEL, J. H., HUH, W. J., SEQUEIRA, I., LOUGH, K. J.,
916 WAGNER, B. L., MARANGONI, P., WATT, F. M., KLEIN, O. D., COFFEY, R. J. &
917 WILLIAMS, S. E. 2019. Heterogeneity within Stratified Epithelial Stem Cell Populations
918 Maintains the Oral Mucosa in Response to Physiological Stress. *Cell Stem Cell,* 25**,** 814-829
919 e6.DOI: 10.1016/j.stem.2019.11.005
920
921 CARROLL, M. C. & ISENMAN, D. E. 2012. Regulation of humoral immunity by
922 complement. *Immunity,* 37**,** 199-207.DOI: 10.1016/j.immuni.2012.08.002
923
924 CASTRO-DOPICO, T., DENNISON, T. W., FERDINAND, J. R., MATHEWS, R. J.,
925 FLEMING, A., CLIFT, D., STEWART, B. J., JING, C., STRONGILI, K., LABZIN, L. I.,
926 MONK, E. J. M., SAEB-PARSY, K., BRYANT, C. E., CLARE, S., PARKES, M. &
927 CLATWORTHY, M. R. 2019. Anti-commensal IgG Drives Intestinal Inflammation and
928 Type 17 Immunity in Ulcerative Colitis. *Immunity,* 50**,** 1099-1114 e10.DOI:
929 10.1016/j.immuni.2019.02.006
930
931 CEKICI, A., KANTARCI, A., HASTURK, H. & VAN DYKE, T. E. 2014. Inflammatory and
932 immune pathways in the pathogenesis of periodontal disease. *Periodontol 2000,* 64**,** 57-
933 80.DOI: 10.1111/prd.12002
934
935 CHAKAROV, S., LIM, H. Y., TAN, L., LIM, S. Y., SEE, P., LUM, J., ZHANG, X. M.,
936 FOO, S., NAKAMIZO, S., DUAN, K., KONG, W. T., GENTEK, R., BALACHANDER, A.,
937 CARBAJO, D., BLERIOT, C., MALLERET, B., TAM, J. K. C., BAIG, S., SHABEER, M.,
938 TOH, S. E. S., SCHLITZER, A., LARBI, A., MARICHAL, T., MALISSEN, B., CHEN, J.,
939 POIDINGER, M., KABASHIMA, K., BAJENOFF, M., NG, L. G., ANGELI, V. &
940 GINHOUX, F. 2019. Two distinct interstitial macrophage populations coexist across tissues
941 in specific subtissular niches. *Science,* 363.DOI: 10.1126/science.aau0964
942
943 CHEN, E. Y., TAN, C. M., KOU, Y., DUAN, Q., WANG, Z., MEIRELLES, G. V., CLARK,
944 N. R. & MA'AYAN, A. 2013. Enrichr: interactive and collaborative HTML5 gene list
945 enrichment analysis tool. *BMC Bioinformatics,* 14**,** 128.DOI: 10.1186/1471-2105-14-128
946
947 CHEN, K., MAGRI, G., GRASSET, E. K. & CERUTTI, A. 2020. Rethinking mucosal
948 antibody responses: IgM, IgG and IgD join IgA. *Nat Rev Immunol,* 20**,** 427-441.DOI:
949 10.1038/s41577-019-0261-1
950
951 CRISAN, M., YAP, S., CASTEILLA, L., CHEN, C. W., CORSELLI, M., PARK, T. S.,
952 ANDRIOLO, G., SUN, B., ZHENG, B., ZHANG, L., NOROTTE, C., TENG, P. N., TRAAS,
953 J., SCHUGAR, R., DEASY, B. M., BADYLAK, S., BUHRING, H. J., GIACOBINO, J. P.,
954 LAZZARI, L., HUARD, J. & PEAULT, B. 2008. A perivascular origin for mesenchymal
955 stem cells in multiple human organs. *Cell Stem Cell,* 3**,** 301-13.DOI:
956 10.1016/j.stem.2008.07.003

CROFT, A. P., CAMPOS, J., JANSEN, K., TURNER, J. D., MARSHALL, J., ATTAR, M., SAVARY, L., WEHMEYER, C., NAYLOR, A. J., KEMBLE, S., BEGUM, J., DURHOLZ, K., PERLMAN, H., BARONE, F., MCGETTRICK, H. M., FEARON, D. T., WEI, K., RAYCHAUDHURI, S., KORSUNSKY, I., BRENNER, M. B., COLES, M., SANSOM, S. N., FILER, A. & BUCKLEY, C. D. 2019. Distinct fibroblast subsets drive inflammation and damage in arthritis. *Nature*.DOI: 10.1038/s41586-019-1263-7

DAMGAARD, C., HOLMSTRUP, P., VAN DYKE, T. E. & NIELSEN, C. H. 2015. The complement system and its role in the pathogenesis of periodontitis: current concepts. *J Periodontal Res,* 50**,** 283-93.DOI: 10.1111/jre.12209

DAVANIAN, H., STRANNEHEIM, H., BAGE, T., LAGERVALL, M., JANSSON, L., LUNDEBERG, J. & YUCEL-LINDBERG, T. 2012. Gene expression profiles in paired gingival biopsies from periodontitis-affected and healthy tissues revealed by massively parallel sequencing. *PLoS One,* 7**,** e46440.DOI: 10.1371/journal.pone.0046440

DEMMER, R. T., BEHLE, J. H., WOLF, D. L., HANDFIELD, M., KEBSCHULL, M., CELENTI, R., PAVLIDIS, P. & PAPAPANOU, P. N. 2008. Transcriptomes in healthy and diseased gingival tissues. *J Periodontol,* 79**,** 2112-24.DOI: 10.1902/jop.2008.080139

DUTZAN, N., KONKEL, J. E., GREENWELL-WILD, T. & MOUTSOPOULOS, N. M. 2016. Characterization of the human immune cell network at the gingival barrier. *Mucosal Immunol,* 9**,** 1163-1172.DOI: 10.1038/mi.2015.136

EFFROS, R. B. & PAWELEC, G. 1997. Replicative senescence of T cells: does the Hayflick Limit lead to immune exhaustion? *Immunol Today,* 18**,** 450-4. DOI:10.1016/s0167-5699(97)01079-7

EISENBARTH, S. C. 2019. Dendritic cell subsets in T cell programming: location dictates function. *Nat Rev Immunol,* 19**,** 89-103.DOI: 10.1038/s41577-018-0088-1

FARBEHI, N., PATRICK, R., DORISON, A., XAYMARDAN, M., JANBANDHU, V., WYSTUB-LIS, K., HO, J. W., NORDON, R. E. & HARVEY, R. P. 2019. Single-cell expression profiling reveals dynamic flux of cardiac stromal, vascular and immune cells in health and injury. *Elife,* 8.DOI: 10.7554/eLife.43882

FIOCCHI, C., INA, K., DANESE, S., LEITE, A. Z. & VOGEL, J. D. 2006. Alterations of mesenchymal and endothelial cells in inflammatory bowel diseases. *Adv Exp Med Biol,* 579**,** 168-76.DOI: 10.1007/0-387-33778-4_11

FRANCOIS, M., CAPRINI, A., HOSKING, B., ORSENIGO, F., WILHELM, D., BROWNE, C., PAAVONEN, K., KARNEZIS, T., SHAYAN, R., DOWNES, M., DAVIDSON, T., TUTT, D., CHEAH, K. S., STACKER, S. A., MUSCAT, G. E., ACHEN, M. G., DEJANA, E. & KOOPMAN, P. 2008. Sox18 induces development of the lymphatic vasculature in mice. *Nature,* 456**,** 643-7.DOI: 10.1038/nature07391

GREICIUS, G., KABIRI, Z., SIGMUNDSSON, K., LIANG, C., BUNTE, R., SINGH, M. K. & VIRSHUP, D. M. 2018. PDGFRalpha(+) pericryptal stromal cells are the critical source of Wnts and RSPO3 for murine intestinal stem cells in vivo. *Proc Natl Acad Sci U S A,* 115**,** E3173-E3181.DOI: 10.1073/pnas.1713510115

GUERRERO-JUAREZ, C. F., DEDHIA, P. H., JIN, S., RUIZ-VEGA, R., MA, D., LIU, Y., YAMAGA, K., SHESTOVA, O., GAY, D. L., YANG, Z., KESSENBROCK, K., NIE, Q., PEAR, W. S., COTSARELIS, G. & PLIKUS, M. V. 2019. Single-cell analysis reveals fibroblast heterogeneity and myeloid-derived adipocyte progenitors in murine skin wounds. *Nat Commun,* 10**,** 650.DOI: 10.1038/s41467-018-08247-x

GULATI, G. S., SIKANDAR, S. S., WESCHE, D. J., MANJUNATH, A., BHARADWAJ, A., BERGER, M. J., ILAGAN, F., KUO, A. H., HSIEH, R. W., CAI, S., ZABALA, M., SCHEEREN, F. A., LOBO, N. A., QIAN, D., YU, F. B., DIRBAS, F. M., CLARKE, M. F. & NEWMAN, A. M. 2020. Single-cell transcriptional diversity is a hallmark of developmental potential. *Science,* 367**,** 405-411.DOI: 10.1126/science.aax0249

HAJISHENGALLIS, G. 2014. Immunomicrobial pathogenesis of periodontitis: keystones, pathobionts, and host response. *Trends Immunol,* 35**,** 3-11.DOI: 10.1016/j.it.2013.09.001

HAJISHENGALLIS, G., LIANG, S., PAYNE, M. A., HASHIM, A., JOTWANI, R., ESKAN, M. A., MCINTOSH, M. L., ALSAM, A., KIRKWOOD, K. L., LAMBRIS, J. D., DARVEAU, R. P. & CURTIS, M. A. 2011. Low-abundance biofilm species orchestrates inflammatory periodontal disease through the commensal microbiota and complement. *Cell Host Microbe,* 10**,** 497-506.DOI: 10.1016/j.chom.2011.10.006

HAJISHENGALLIS, G., REIS, E. S., MASTELLOS, D. C., RICKLIN, D. & LAMBRIS, J. D. 2017. Novel mechanisms and functions of complement. *Nat Immunol,* 18**,** 1288-1298.DOI: 10.1038/ni.3858

HAN, X., ZHOU, Z., FEI, L., SUN, H., WANG, R., CHEN, Y., CHEN, H., WANG, J., TANG, H., GE, W., ZHOU, Y., YE, F., JIANG, M., WU, J., XIAO, Y., JIA, X., ZHANG, T., MA, X., ZHANG, Q., BAI, X., LAI, S., YU, C., ZHU, L., LIN, R., GAO, Y., WANG, M., WU, Y., ZHANG, J., ZHAN, R., ZHU, S., HU, H., WANG, C., CHEN, M., HUANG, H., LIANG, T., CHEN, J., WANG, W., ZHANG, D. & GUO, G. 2020. Construction of a human cell landscape at single-cell level. *Nature,* 581**,** 303-309.DOI: 10.1038/s41586-020-2157-4

HELLSTROM, M., GERHARDT, H., KALEN, M., LI, X., ERIKSSON, U., WOLBURG, H. & BETSHOLTZ, C. 2001. Lack of pericytes leads to endothelial hyperplasia and abnormal vascular morphogenesis. *J Cell Biol,* 153**,** 543-53.DOI: 10.1083/jcb.153.3.543

JAMES, K. R., GOMES, T., ELMENTAITE, R., KUMAR, N., GULLIVER, E. L., KING, H. W., STARES, M. D., BAREHAM, B. R., FERDINAND, J. R., PETROVA, V. N., POLANSKI, K., FORSTER, S. C., JARVIS, L. B., SUCHANEK, O., HOWLETT, S., JAMES, L. K., JONES, J. L., MEYER, K. B., CLATWORTHY, M. R., SAEB-PARSY, K., LAWLEY, T. D. & TEICHMANN, S. A. 2020. Distinct microbial and immune niches of the human colon. *Nat Immunol,* 21**,** 343-353.DOI: 10.1038/s41590-020-0602-z

JONES, K. B., FURUKAWA, S., MARANGONI, P., MA, H., PINKARD, H., D'URSO, R., ZILIONIS, R., KLEIN, A. M. & KLEIN, O. D. 2019. Quantitative Clonal Analysis and Single-Cell Transcriptomics Reveal Division Kinetics, Hierarchy, and Fate of Oral Epithelial Progenitor Cells. *Cell Stem Cell,* 24**,** 183-192 e8.DOI: 10.1016/j.stem.2018.10.015

JONES, N., ILJIN, K., DUMONT, D. J. & ALITALO, K. 2001. Tie receptors: new modulators of angiogenic and lymphangiogenic responses. *Nat Rev Mol Cell Biol,* 2**,** 257-67.DOI: 0.1038/35067005

KABIRI, Z., GREICIUS, G., MADAN, B., BIECHELE, S., ZHONG, Z., ZARIBAFZADEH, H., EDISON, ALIYEV, J., WU, Y., BUNTE, R., WILLIAMS, B. O., ROSSANT, J. & VIRSHUP, D. M. 2014. Stroma provides an intestinal stem cell niche in the absence of epithelial Wnts. *Development,* 141**,** 2206-15.DOI: 10.1242/dev.104976

KIM, J. E., FEI, L., YIN, W. C., COQUENLORGE, S., RAO-BHATIA, A., ZHANG, X., SHI, S. S. W., LEE, J. H., HAHN, N. A., RIZVI, W., KIM, K. H., SUNG, H. K., HUI, C. C., GUO, G. & KIM, T. H. 2020. Single cell and genetic analyses reveal conserved populations and signaling mechanisms of gastrointestinal stromal niches. *Nat Commun,* 11**,** 334.DOI: 10.1038/s41467-019-14058-5

KIM, Y. G., KIM, M., KANG, J. H., KIM, H. J., PARK, J. W., LEE, J. M., SUH, J. Y., KIM, J. Y., LEE, J. H. & LEE, Y. 2016. Transcriptome sequencing of gingival biopsies from chronic periodontitis patients reveals novel gene expression and splicing patterns. *Hum Genomics,* 10**,** 28.DOI: 10.1186/s40246-016-0084-0

KINANE, D. F. 2001. Causation and pathogenesis of periodontal disease. *Periodontol 2000,* 25**,** 8-20.DOI: 10.1034/j.1600-0757.2001.22250102.x

KINANE, D. F., LAPPIN, D. F., KOULOURI, O. & BUCKLEY, A. 1999. Humoral immune responses in periodontal disease may have mucosal and systemic immune features. *Clin Exp Immunol,* 115**,** 534-41.DOI: 10.1046/j.1365-2249.1999.00819.x

KINCHEN, J., CHEN, H. H., PARIKH, K., ANTANAVICIUTE, A., JAGIELOWICZ, M., FAWKNER-CORBETT, D., ASHLEY, N., CUBITT, L., MELLADO-GOMEZ, E., ATTAR, M., SHARMA, E., WILLS, Q., BOWDEN, R., RICHTER, F. C., AHERN, D., PURI, K. D., HENAULT, J., GERVAIS, F., KOOHY, H. & SIMMONS, A. 2018. Structural Remodeling of the Human Colonic Mesenchyme in Inflammatory Bowel Disease. *Cell,* 175**,** 372-386 e17.`doi: 10.1016/j.cell.2018.08.067

KRAMANN, R., SCHNEIDER, R. K., DIROCCO, D. P., MACHADO, F., FLEIG, S., BONDZIE, P. A., HENDERSON, J. M., EBERT, B. L. & HUMPHREYS, B. D. 2015. Perivascular Gli1+ progenitors are key contributors to injury-induced organ fibrosis. *Cell Stem Cell,* 16**,** 51-66.DOI: 10.1016/j.stem.2014.11.004

KRAUSGRUBER, T., FORTELNY, N., FIFE-GERNEDL, V., SENEKOWITSCH, M., SCHUSTER, L. C., LERCHER, A., NEMC, A., SCHMIDL, C., RENDEIRO, A. F., BERGTHALER, A. & BOCK, C. 2020. Structural cells are key regulators of organ-specific immune responses. *Nature*.DOI: 10.1038/s41586-020-2424-4

KRISHNAN, S., PRISE, I. E., WEMYSS, K., SCHENCK, L. P., BRIDGEMAN, H. M., MCCLURE, F. A., ZANGERLE-MURRAY, T., O'BOYLE, C., BARBERA, T. A., MAHMOOD, F., BOWDISH, D. M. E., ZAISS, D. M. W., GRAINGER, J. R. & KONKEL, J. E. 2018. Amphiregulin-producing gammadelta T cells are vital for safeguarding oral barrier immune homeostasis. *Proc Natl Acad Sci U S A,* 115**,** 10738-10743.DOI: 10.1073/pnas.1802320115

KUHN, B., DEL MONTE, F., HAJJAR, R. J., CHANG, Y. S., LEBECHE, D., ARAB, S. & KEATING, M. T. 2007. Periostin induces proliferation of differentiated cardiomyocytes and promotes cardiac repair. *Nat Med,* 13**,** 962-9.DOI: 10.1038/nm1619

LAMBRECHTS, D., WAUTERS, E., BOECKX, B., AIBAR, S., NITTNER, D., BURTON, O., BASSEZ, A., DECALUWE, H., PIRCHER, A., VAN DEN EYNDE, K., WEYNAND, B., VERBEKEN, E., DE LEYN, P., LISTON, A., VANSTEENKISTE, J., CARMELIET, P., AERTS, S. & THIENPONT, B. 2018. Phenotype molding of stromal cells in the lung tumor microenvironment. *Nat Med,* 24**,** 1277-1289.DOI: 10.1038/s41591-018-0096-5

LAMONT, R. J. & HAJISHENGALLIS, G. 2015. Polymicrobial synergy and dysbiosis in inflammatory disease. *Trends Mol Med,* 21**,** 172-83.DOI: 10.1016/j.molmed.2014.11.004

LINDBLOM, P., GERHARDT, H., LIEBNER, S., ABRAMSSON, A., ENGE, M., HELLSTROM, M., BACKSTROM, G., FREDRIKSSON, S., LANDEGREN, U., NYSTROM, H. C., BERGSTROM, G., DEJANA, E., OSTMAN, A., LINDAHL, P. & BETSHOLTZ, C. 2003. Endothelial PDGF-B retention is required for proper investment of pericytes in the microvessel wall. *Genes Dev,* 17**,** 1835-40.DOI: 10.1101/gad.266803

LINDHE, J., KARRING, T. & LANG, N. P. 2008. *Clinical periodontology and implant dentistry,* Oxford, Blackwell Munksgaard.

LUNDMARK, A., DAVANIAN, H., BAGE, T., JOHANNSEN, G., KORO, C., LUNDEBERG, J. & YUCEL-LINDBERG, T. 2015. Transcriptome analysis reveals mucin 4 to be highly associated with periodontitis and identifies pleckstrin as a link to systemic diseases. *Sci Rep,* 5**,** 18475.DOI: 10.1038/srep18475

LUNDMARK, A., GERASIMCIK, N., BAGE, T., JEMT, A., MOLLBRINK, A., SALMEN, F., LUNDEBERG, J. & YUCEL-LINDBERG, T. 2018. Gene expression profiling of periodontitis-affected gingival tissue by spatial transcriptomics. *Sci Rep,* 8**,** 9370.DOI: 10.1038/s41598-018-27627-3

MAEKAWA, T., KRAUSS, J. L., ABE, T., JOTWANI, R., TRIANTAFILOU, M., TRIANTAFILOU, K., HASHIM, A., HOCH, S., CURTIS, M. A., NUSSBAUM, G., LAMBRIS, J. D. & HAJISHENGALLIS, G. 2014. Porphyromonas gingivalis manipulates complement and TLR signaling to uncouple bacterial clearance from inflammation and promote dysbiosis. *Cell Host Microbe,* 15**,** 768-78.DOI: 10.1016/j.chom.2014.05.012

MAHANONDA, R., CHAMPAIBOON, C., SUBBALEKHA, K., SA-ARD-IAM, N., RATTANATHAMMATADA, W., THAWANAPHONG, S., RERKYEN, P., YOSHIMURA, F., NAGANO, K., LANG, N. P. & PICHYANGKUL, S. 2016. Human Memory B Cells in Healthy Gingiva, Gingivitis, and Periodontitis. *J Immunol,* 197**,** 715-25.DOI: 10.4049/jimmunol.1600540

MEYERS, C. A., XU, J., ZHANG, L., ASATRIAN, G., DING, C., YAN, N., BRODERICK, K., SACKS, J., GOYAL, R., ZHANG, X., TING, K., PEAULT, B., SOO, C. & JAMES, A. W. 2018. Early Immunomodulatory Effects of Implanted Human Perivascular Stromal Cells During Bone Formation. *Tissue Eng Part A,* 24**,** 448-457.DOI: 10.1089/ten.TEA.2017.0023

NOWARSKI, R., JACKSON, R. & FLAVELL, R. A. 2017. The Stromal Intervention: Regulation of Immunity and Inflammation at the Epithelial-Mesenchymal Barrier. *Cell,* 168**,** 362-375.DOI: 10.1016/j.cell.2016.11.040

OGURA, S., KURATA, K., HATTORI, Y., TAKASE, H., ISHIGURO-OONUMA, T., HWANG, Y., AHN, S., PARK, I., IKEDA, W., KUSUHARA, S., FUKUSHIMA, Y., NARA, H., SAKAI, H., FUJIWARA, T., MATSUSHITA, J., EMA, M., HIRASHIMA, M., MINAMI, T., SHIBUYA, M., TAKAKURA, N., KIM, P., MIYATA, T., OGURA, Y. & UEMURA, A. 2017. Sustained inflammation after pericyte depletion induces irreversible blood-retina barrier breakdown. *JCI Insight,* 2**,** e90905.DOI: 10.1172/jci.insight.90905

OLIVER-BELL, J., BUTCHER, J. P., MALCOLM, J., MACLEOD, M. K., ADRADOS PLANELL, A., CAMPBELL, L., NIBBS, R. J., GARSIDE, P., MCINNES, I. B. & CULSHAW, S. 2015. Periodontitis in the absence of B cells and specific anti-bacterial antibody. *Mol Oral Microbiol,* 30**,** 160-9.DOI: 10.1111/omi.12082

PEYSER, R., MACDONNELL, S., GAO, Y., CHENG, L., KIM, Y., KAPLAN, T., RUAN, Q., WEI, Y., NI, M., ADLER, C., ZHANG, W., DEVALARAJA-NARASHIMHA, K., GRINDLEY, J., HALASZ, G. & MORTON, L. 2019. Defining the Activated Fibroblast Population in Lung Fibrosis Using Single-Cell Sequencing. *Am J Respir Cell Mol Biol,* 61**,** 74-85.DOI: 10.1165/rcmb.2018-0313OC

PIHLSTROM, B. L., MICHALOWICZ, B. S. & JOHNSON, N. W. 2005. Periodontal diseases. *Lancet,* 366**,** 1809-20.DOI: 10.1016/S0140-6736(05)67728-8

SACCHETTI, B., FUNARI, A., REMOLI, C., GIANNICOLA, G., KOGLER, G., LIEDTKE, S., COSSU, G., SERAFINI, M., SAMPAOLESI, M., TAGLIAFICO, E., TENEDINI, E., SAGGIO, I., ROBEY, P. G., RIMINUCCI, M. & BIANCO, P. 2016. No Identical "Mesenchymal Stem Cells" at Different Times and Sites: Human Committed Progenitors of Distinct Origin and Differentiation Potential Are Incorporated as Adventitial Cells in Microvessels. *Stem Cell Reports,* 6**,** 897-913.DOI: 10.1016/j.stemcr.2016.05.011

SCHINDELIN, J., ARGANDA-CARRERAS, I., FRISE, E., KAYNIG, V., LONGAIR, M., PIETZSCH, T., PREIBISCH, S., RUEDEN, C., SAALFELD, S., SCHMID, B., TINEVEZ, J. Y., WHITE, D. J., HARTENSTEIN, V., ELICEIRI, K., TOMANCAK, P. & CARDONA, A. 2012. Fiji: an open-source platform for biological-image analysis. *Nat Methods,* 9**,** 676-82.DOI: 10.1038/nmeth.2019

SHOSHKES-CARMEL, M., WANG, Y. J., WANGENSTEEN, K. J., TOTH, B., KONDO, A., MASSASA, E. E., ITZKOVITZ, S. & KAESTNER, K. H. 2018. Subepithelial telocytes are an important source of Wnts that supports intestinal crypts. *Nature,* 557**,** 242-246.DOI: 10.1038/s41586-018-0084-4

STUART, T., BUTLER, A., HOFFMAN, P., HAFEMEISTER, C., PAPALEXI, E., MAUCK, W. M., 3RD, HAO, Y., STOECKIUS, M., SMIBERT, P. & SATIJA, R. 2019. Comprehensive Integration of Single-Cell Data. *Cell,* 177**,** 1888-1902 e21.DOI: 10.1016/j.cell.2019.05.031

TABIB, T., MORSE, C., WANG, T., CHEN, W. & LAFYATIS, R. 2018. SFRP2/DPP4 and FMO1/LSP1 Define Major Fibroblast Populations in Human Skin. *J Invest Dermatol,* 138**,** 802-810.DOI: 10.1016/j.jid.2017.09.045

TAKEDA, N., JAIN, R., LEBOEUF, M. R., PADMANABHAN, A., WANG, Q., LI, L., LU, M. M., MILLAR, S. E. & EPSTEIN, J. A. 2013. Hopx expression defines a subset of multipotent hair follicle stem cells and a progenitor population primed to give rise to K6+ niche cells. *Development,* 140**,** 1655-64.DOI: 10.1242/dev.093005

TAKEDA, N., JAIN, R., LEBOEUF, M. R., WANG, Q., LU, M. M. & EPSTEIN, J. A. 2011. Interconversion between intestinal stem cell populations in distinct niches. *Science,* 334**,** 1420-4.DOI: 10.1126/science.1213214

TESCHENDORFF, A. E. & ENVER, T. 2017. Single-cell entropy for accurate estimation of differentiation potency from a cell's transcriptome. *Nat Commun,* 8**,** 15599.DOI: 10.1038/ncomms15599

THORBERT-MROS, S., LARSSON, L. & BERGLUNDH, T. 2015. Cellular composition of long-standing gingivitis and periodontitis lesions. *J Periodontal Res,* 50**,** 535-43.DOI: 10.1111/jre.12236

TOMASEK, J. J., GABBIANI, G., HINZ, B., CHAPONNIER, C. & BROWN, R. A. 2002. Myofibroblasts and mechano-regulation of connective tissue remodelling. *Nat Rev Mol Cell Biol,* 3**,** 349-63.DOI: 10.1038/nrm809

TUMBAR, T., GUASCH, G., GRECO, V., BLANPAIN, C., LOWRY, W. E., RENDL, M. & FUCHS, E. 2004. Defining the epithelial stem cell niche in skin. *Science,* 303**,** 359-63.DOI: 10.1126/science.1092436

VALLEJO, A. N., WEYAND, C. M. & GORONZY, J. J. 2004. T-cell senescence: a culprit of immune abnormalities in chronic inflammation and persistent infection. *Trends Mol Med,* 10**,** 119-24.DOI: 10.1016/j.molmed.2004.01.002

WHITFIELD, M. L., GEORGE, L. K., GRANT, G. D. & PEROU, C. M. 2006. Common markers of proliferation. *Nat Rev Cancer,* 6**,** 99-106.DOI: 10.1038/nrc1802

XIE, T., WANG, Y., DENG, N., HUANG, G., TAGHAVIFAR, F., GENG, Y., LIU, N., KULUR, V., YAO, C., CHEN, P., LIU, Z., STRIPP, B., TANG, J., LIANG, J., NOBLE, P. W. & JIANG, D. 2018. Single-Cell Deconvolution of Fibroblast Heterogeneity in Mouse Pulmonary Fibrosis. *Cell Rep,* 22**,** 3625-3640.DOI: 10.1016/j.celrep.2018.03.010

YIANNI, V. & SHARPE, P. T. 2018. Molecular Programming of Perivascular Stem Cell Precursors. *Stem Cells,* 36**,** 1890-1904.DOI: 10.1002/stem.2895

YUCEL-LINDBERG, T. & BAGE, T. 2013. Inflammatory mediators in the pathogenesis of periodontitis. *Expert Rev Mol Med,* 15**,** e7.DOI: 10.1017/erm.2013.8

ZAIDI, M. 2007. Skeletal remodeling in health and disease. *Nat Med,* 13**,** 791-801.DOI: 10.1038/nm1593

ZHANG, H. Y. & PHAN, S. H. 1999. Inhibition of myofibroblast apoptosis by transforming growth factor beta(1). *Am J Respir Cell Mol Biol,* 21**,** 658-65.DOI: 10.1165/ajrcmb.21.6.3720

ZOELLNER, H., CHAPPLE, C. C. & HUNTER, N. 2002. Microvasculature in gingivitis and chronic periodontitis: disruption of vascular networks with protracted inflammation. *Microsc Res Tech,* 56**,** 15-31.DOI: 10.1002/jemt.10009

SUPPLEMENTARY INFORMATION

SUPPLEMENTARY FIGURES

SUPPLEMENTARY FIGURE 1. Single-cell profiling of healthy human gingiva datasets using 10x Chromium, Related to Figure 1.

SUPPLEMENTARY FIGURE 2. Single-cell profiling of healthy and disease human gingiva using 10x Chromium, Related to Figure 1.

SUPPLEMENTARY FIGURE 3. Re-clustering of human stromal gingival cells in health and disease, Related to Figure 3.

SUPPLEMENTARY FIGURE 4. Re-clustering of human epithelial gingival cells in health and disease, Related to Figure 4.

SUPPLEMENTARY FIGURE 5. Flow Cytometry Gating Strategies on Human Gingival Cells.

Supplementary Figure 1. Single-cell profiling of healthy human gingiva datasets using 10x Chromium, Related to Figure 1.

A. UMAP visualisation of human gingiva clusters from healthy human donors.

B. Scatter plots showing differential expressed genes across the two healthy samples. Panels A-B, n=2 individuals.

Figure S1

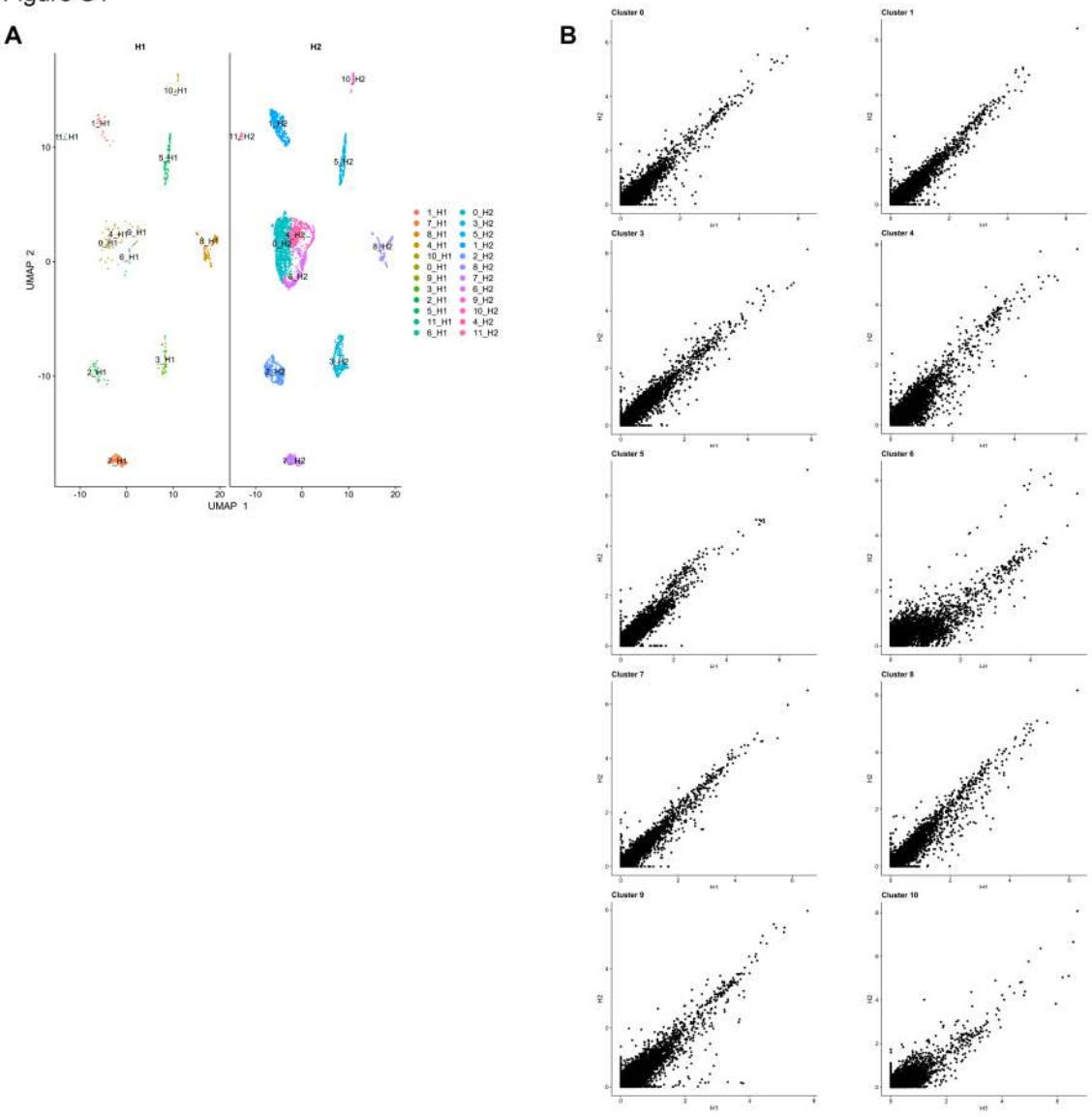

Supplementary Figure 2. Single-cell profiling of healthy and disease human gingiva using 10x Chromium, Related to Figure 1.

A. UMAP illustration of scRNA-seq data obtained from healthy and periodontitis cells (n= 12,411) from four donors coloured by condition.

B. Feature Plot showing the expression of lineage marker genes used for cell-type classification.

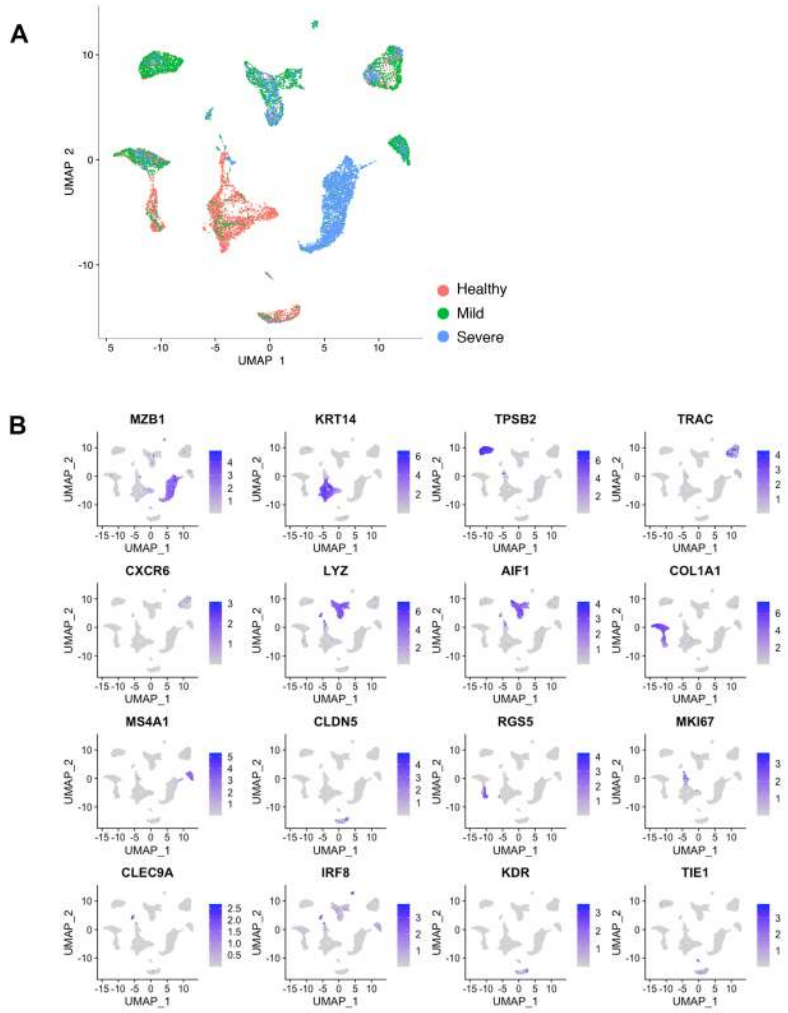

Supplementary Figure 3. Re-clustering of human stromal gingival cells in health and disease, Related to Figure 2.

A. Feature Plots showing the expression of individual genes used for cell-type assignment of different stromal subsets.

B. GO enrichment terms for the different stromal subsets. -log adjusted p-value shown (dotted line corresponds to FDR = 0.05).

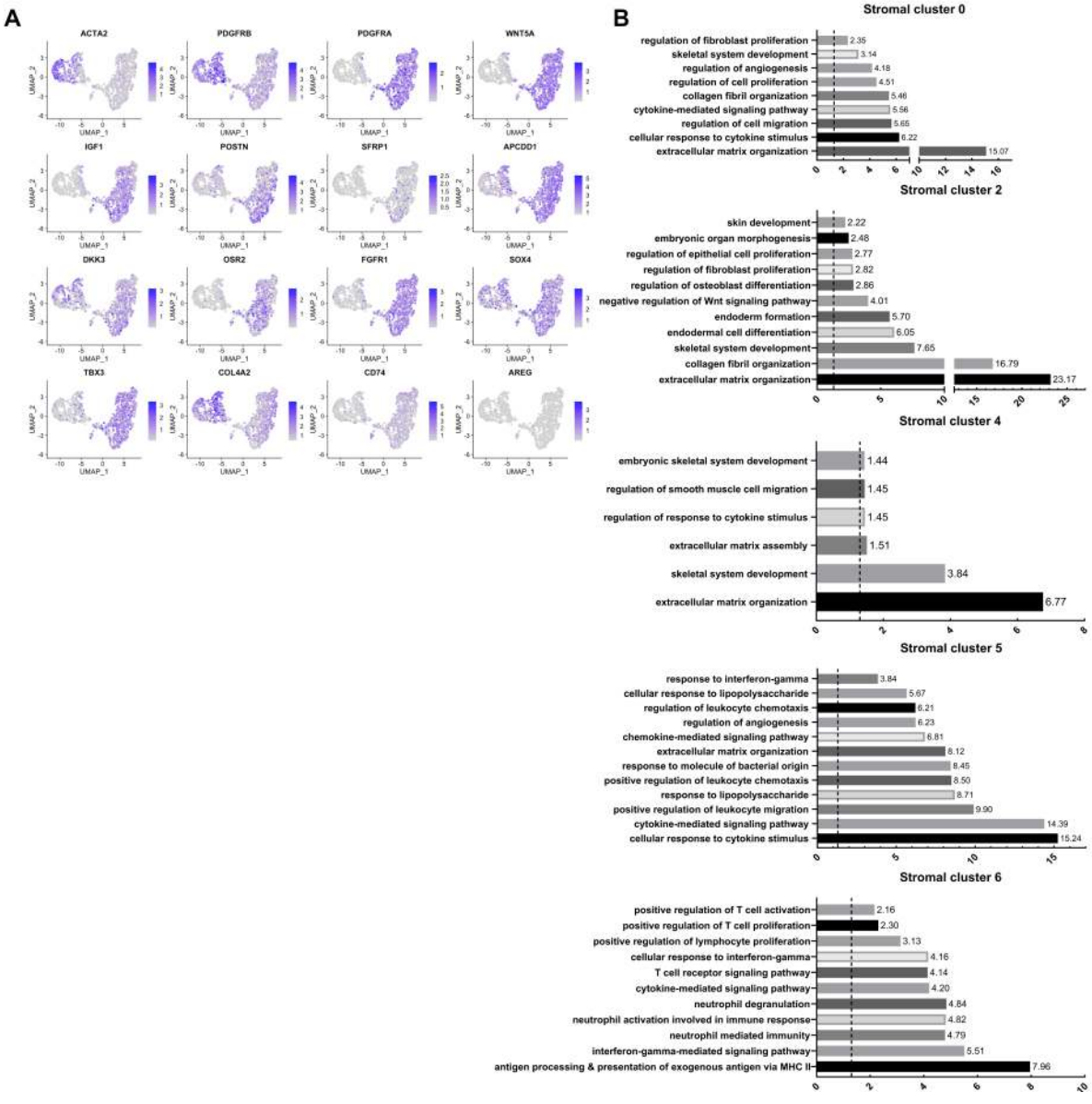

Supplementary Figure 4. Re-clustering of human epithelial gingival cells in health and disease, Related to Figure 3.

A. Feature Plots showing the expression of individual genes used for cell-type assignment of different epithelial subsets.

B. GO enrichment terms for the different epithelial subsets. -log adjusted p-value shown (dotted line corresponds to FDR = 0.05).

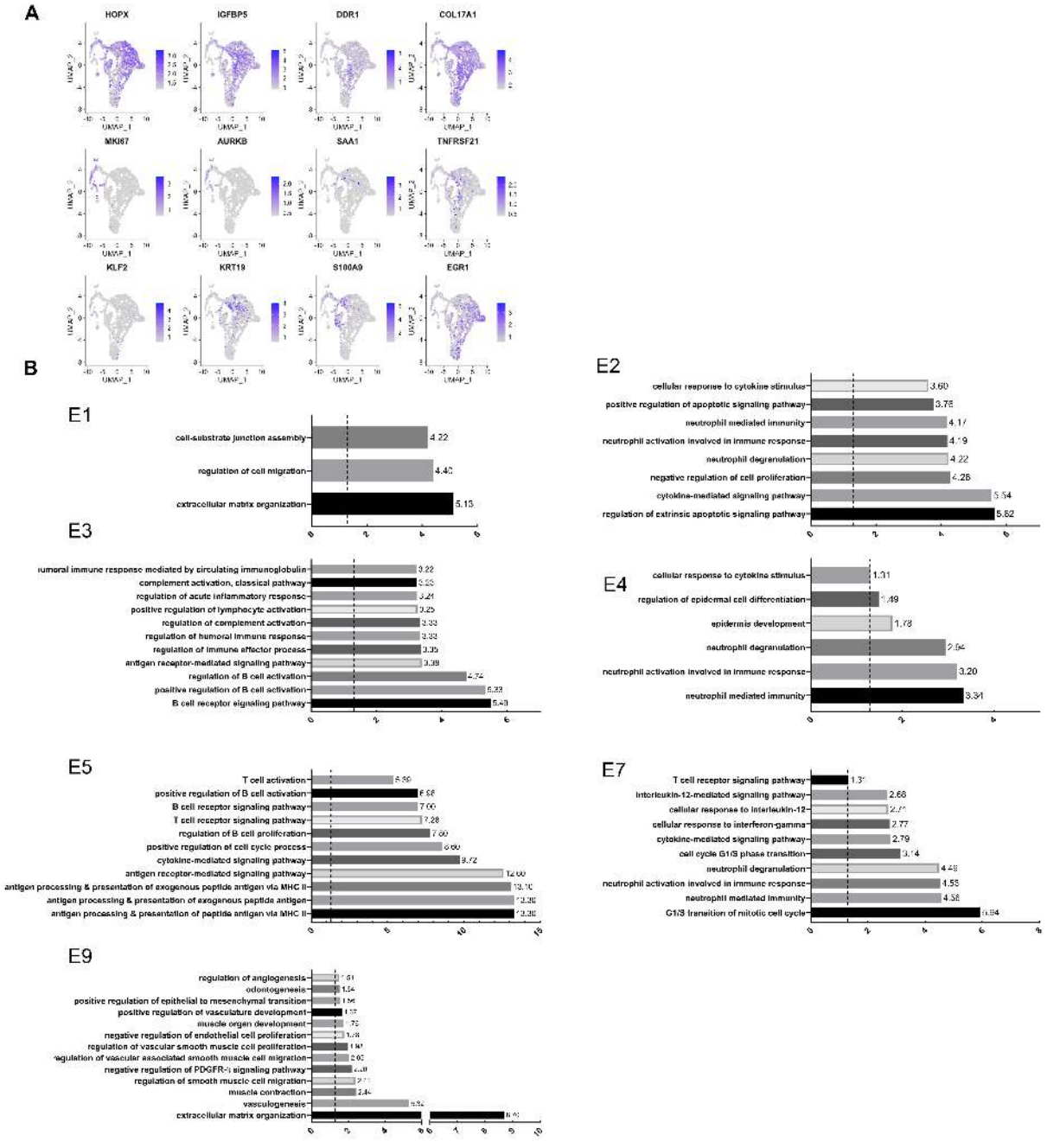

Supplementary Figure 5. Flow Cytometry Gating Strategies on Human Gingival Cells.